Particulate antigens administrated by intranasal and intravaginal routes in a prime-boost strategy improve HIV-specific TFH generation, high-quality antibodies and long-lasting mucosal immunity

Thomas Vazquez, Léa Torrieri-Damard, Fabien Pitoiset, Béatrice Levacher, James Vigneron, Luzia Mayr, Faustine Brimaud, Benjamin Bonnet, Christiane Moog, David Klatzmann, et al.

Particulate antigens administrated by intranasal and intravaginal routes in a prime-boost strategy improve HIV-specific T_{FH} generation, high-quality antibodies and long-lasting mucosal immunity

Thomas Vazquez [1, 2], Léa Torrieri-Damard [1, 2], Fabien Pitoiset [1, 2, 3], Béatrice Levacher [1, 2], James Vigneron [1, 2], Luzia Mayr [4], Faustine Brimaud [1, 2], Benjamin Bonnet [1, 2, 3], Christiane Moog [4], David Klatzmann [1, 2, 3], Bertrand Bellier [1, 2, 3 *].

[1] Sorbonne Université, UMRS 959, laboratory I[3], F-75013, Paris, France

[2] INSERM, UMRS 959, laboratory I[3], F-75013, Paris, France

[3] AP-HP, Groupe Hospitalier Pitié-Salpêtrière, Department of Biotherapies and the Clinical Investigation Center in Biotherapy, F-75013, Paris, France

[4] Université de Strasbourg, Fédération de médecine Translationnelle de Strasbourg, INSERM U1109, F-67000, France

Corresponding author: bertrand.bellier@sorbonne-universite.fr

Abstract

Mucosal surfaces serve as the primary portal of entry for pathogens like SARS-CoV-2 coronavirus or HIV in the human body. Mucosal vaccination may be critical to successfully induce long-lasting systemic and local immune responses to confer sterilizing immunity. However, antigen formulations and delivery methods must be properly selected since they are decisive for the quality and the magnitude of the elicited immune responses in mucosa. We addressed the importance of the particulate form of the antigen for mucosal vaccination by comparing VLP- or protein-based vaccines in a mouse model.

Based on a mucosal prime-boost immunization protocol combining (i) HIV-pseudotyped recombinant VLPs (HIV-VLPs) and (ii) plasmid DNA encoding HIV- VLPs (pVLPs), we demonstrated that combination of intranasal primes and intravaginal boosts is optimal to elicit both humoral and cellular memory responses in mucosa. Interestingly, our results show that in contrast to proteins, particulate antigens induce high-quality humoral responses characterized by a high breadth, long-term neutralizing activity and cross-clade reactivity, accompanying with high T follicular helper cell (T_{FH}) response.

These results demonstrate the potential of a VLP-based vaccine to efficiently generate HIV-specific long-lasting immunity and point out the specific role of particulate form of the antigen to drive high-quality mucosal immune responses.

Introduction

Over 35 years have passed since the discovery of human immunodeficiency virus-1 (HIV-1)[1]. Despite significant advancements in prevention and anti-retroviral therapies, the development of an effective and safe vaccine remains a crucial medical priority for successfully managing the pandemic. While the RV144 trial in Thailand demonstrated limited efficacy[2], a vaccine candidate with proven success has yet to be established. Recent findings indicate that the ALVAC/gp120 regimen, despite previous evidence of immunogenicity, did not effectively prevent HIV infection in South Africans[3]. Consequently, major efforts should be made to improve HIV antigens and identifying delivery platforms that can optimally elicit an immune response.

Nanoparticles [4,5], virosomes[6] and virus-like particles[5,7–9] (VLPs) appear to be relevant as they are capable of conformationally displaying antigens on their surfaces, thereby mimicking the native structure of HIV-1 Env. Particularly, VLPs, which are virus-derived structures made up of one or more different molecules with the ability to self-assemble, mimick the form and size of actual virus particles. Beyond their application as vaccines against the authentic virus (e.g., HIV-derived VLPs), VLPs also serve as versatile platforms for displaying vaccine antigens (e.g., HIV-pseudotyped VLPs). Thus, enveloped VLPs are highly attractive vaccine candidates due to their accurate mimicry of wild-type viral particles[7,8,10] and their ability to display HIV-1 functional spikes that contribute to induce neutralizing antibodies. In addition to being good stimulators of innate and acquired immune responses, VLPs are also ideal mucosal vaccines candidates due to the particulate nature and size that promote their uptake in mucosa.

Mucosal surfaces provide a remarkably effective barrier against pathogens. Therefore, enhancing mucosal immunity through vaccines to fortify this initial line of defense holds potential for combating HIV-1. In fact, the preponderance of new HIV infections occur

through the genital and rectal mucosa[11]. Blocking the virus at the portal of entry for infection is currently regarded as the most effective approach with a reduced risk of HIV acquisition. Mucosa-associated lymphoid tissue (MALT) exhibits distinctive characteristics including secretory IgA antibodies (SIgA) which play a crucial role as an initial line of defense[12,13]. The protective role of mucosal antibodies has been highlighted in highly exposed persistently seronegative individuals in which HIV-specific SIgA level in vaginal secretions was correlated with the HIV resistance[14–16]. Induction of local HIV-specific immune responses, including SIgA but also CD8+ and CD4+ T cells seems to be crucial for effective control of natural HIV infection and shaping the course of the disease[17,18]. Nonetheless, developing effective vaccines to prevent HIV transmission through mucosal routes presents a substantial challenge.

Both delivery routes and antigen formulations must be properly selected to induce local immunity. Various routes of immunizations have been considered, but targeting mucosa that is concerned by HIV transmission, i.e. vaginal[6,19,20] or rectal[21] mucosa, is preferred. Alternatively, targeting more easily accessible routes, like intranasal administration, could be more suitable for the general public and has the potential to trigger specific immunity at the cervico-vaginal mucosa[22–25]. Importantly, it has been shown that immunizing nonhuman primates through a combination of intranasal and intramuscular administration routes resulted in complete protection against repeated SHIV vaginal challenges, in contrast to intramuscular vaccination[6].

In this context, we have developed a vaccine platform based on VLPs derived from murine leukemia virus (MLV). These VLPs consist of Moloney MLV-Gag capsid proteins that self-assemble into pseudo-particles within host cells through a process of budding at the plasma membrane. The insertion of target antigens onto these particles can be achieved either by fusing them with Gag proteins or by utilizing membrane

anchors such as the transmembrane domain (TM) of the vesicular stomatitis virus glycoprotein (VSV-G) or the glycosylphosphatidylinositol (GPI)-binding sequence[10]. We previously demonstrated that expression of antigens in/onto VLPs improves significantly their immunogenicity, favouring the generation of both B- and T-cell mediated immune responses, particularly in the context of DNA vaccination[26–28].

Here, we designed HIV-pseudotyped VLP-based vaccines and we established a specific mucosal immunization protocol that combines DNA and VLP in prime-boost strategy to induce both systemic and mucosal-specific immunity in mice. Notably, we point out here the role of particulate antigens in establishing “high-quality” systemic and mucosal immunity. Within this manuscript, VLPs and pVLPs refer to Virus-Like Particles and DNA plasmids encoding Virus-Like Particles respectively. To elaborate further, HIV-VLPs and HIV-pVLPs specifically indicate VLPs or pVLPs pseudotyped with HIV envelope. This envelope can consist of either the wild-type gp160 or the $gp140_{TM}$ variant, which has been modified to include (i) a mutated furin cleavage site (SEKS) to enhance its stability and (ii) a transmembrane (TM) domain from VSV-G to augment its expression onto the pseudotyped VLPs.

Results

HIV-pseudotyped recombinant VLPs and comparison of routes of administration

We designed a $gp140_{TM}$ chimeric form of HIV-1 envelope glycoproteins to increase the antigen expression onto VLPs. The $gp140_{TM}$ sequence derives from the full-length gp160 from the JRFL strain (clade B) in which the transmembrane and cytoplasmic (TM, CT) domain sequences have been replaced by those of the VSV-G (Figure 1A). We showed that the $gp140_{TM}$ chimeric protein is well expressed onto VLPs since

gp120- and gp41-specific antibodies detect the protein showed by Western-Blot. Furthermore, we can infer the presence of functionally folded HIV glycoproteins, given that $gp140_{TM}$-pseudotyped VLPs exhibited binding to human CD4+ T-cells while not binding to CD8+ T-cells (Figure S1). More importantly, we detected an increased expression of gp120 onto $gp140_{TM}$-VLPs compared to gp160-VLPs associated with an improvement of their immunogenicity as shown by the higher level of antibody responses induced after subcutaneous vaccination compared to the native gp160-pseudotyped VLPs (Figure S1).

Using this $gp140_{TM}$ recombinant immunogen, we sought to determine the efficacy of mucosal vaccination in prime-boost strategies combining VLPs and plasmid DNA encoding VLPs (pVLPs; for priming). Mice were primed twice with HIV-pVLPs and boosted twice with HIV-VLPs. We compared both mucosal and parenteral immunization regimens, using a combination of (i) intranasal (IN) or intradermal + electroporation (ID+EP) injections for pVLPs and (ii) intravaginal (IVag) or subcutaneous (SC) injections for VLPs (Figure 1B). As expected, we observed that parenteral route induced higher systemic T-cell immune responses than mucosal route, as evidenced by TNF-α secreting cells within the CD4+ T-cell population and the IFN-γ secreting cells with the CD8+ cells (Figure S2). Additionally, a greater degree of T-cell polyfunctionality was noted in CD4+ cells compared to the mucosal route, as illustrated in the spleen (Figure 1C, D). In contrast, mucosal administrations of vaccines induced significantly higher T-cell responses in both vaginal mucosa and draining lymph nodes (paLN), while parenteral vaccination induced a weak and not significant response in the mucosa (Figure 1C). These results confirm the importance to deliver antigen by mucosal route to induce efficient vaginal HIV-specific T-cell responses.

Likewise, higher systemic IgG antibody responses were observed after parenteral immunizations, but mucosal vaccinations induced significantly higher IgA responses in both systemic and mucosal compartments as shown in serum and vaginal washes respectively (Figure 1E). The similar profiles of IgG responses observed in vagina may be explained by the passive IgG transudation from serum. More importantly, we showed that both parenteral and mucosal immunizations induced systemic neutralizing antibody responses, but only mucosal immunizations could induce vaginal antibodies with neutralizing activity (Figure 1F).

Impact of mucosal priming

We deciphered the role of each route of immunization in prime- (Figure S3) and heterologous prime-boost (Figure 2) strategies to induce mucosal immune responses, by comparing IN and ID+EP immunizations. To note, DNA expression is 2000-fold higher after ID than IN route, based on bioluminescence analysis subsequent to the administration of 10 µg of a plasmid encoding Luciferase (Figure S3). Mice were primed twice with pVLPs and HIV-specific immune responses were analysed two weeks after the last injection. We showed that ID vaccination induced efficient systemic immunity but low distant mucosal responses, highlighting the boost requirement to improve immunity. When the groups were boosted with HIV-VLPs by IVag route (Figure 2A), we observed high frequencies of activated T cells in spleen, paLN and in the vaginal mucosa, with no significant differences of TNF-α (Figure 2B) or IFN-γ secretion (Figure S2) between the two groups. However, significant higher IgA responses in vaginal washes and serum as well as trend higher numbers of IgG-secreting B cells in paLN and IgA-secreting B cells in genital tract were detected in mucosal-primed (IN) mice compared to parenteral (ID) mice (Figure 2C, D). Altogether, these results highlighted the importance of IN primes to initiate the mucosal immunity

in genital tract, especially the establishment of memory B cells in vagina that could be boosted for IgA production after local antigen administration.

Impact of mucosal boosting

We next evaluated the impact of the mucosal boosts assessing the systemic and local antibody responses induced after VLP administration by IVag or intrarectal (IR) routes (Figure 3A). We observed that mucosal administration of VLPs amplified largely the level of HIV-specific IgG in sera, feces and vaginal washes in comparison with non-boosted mice (Figure 3B-D). In contrast, only local boosts elicited mucosal immune responses in the targeted tissue, as shown by high IgA-levels and -antibody secreting cells (ASC) in vagina after intravaginal boosts (Figure 3D-E) and high IgA ASC in colonic mucosa after intrarectal boosts (Figure 3E). In addition to enhancing the antibody response, we were also able to observe an augmentation of the antigen-specific T cell response in systemic compartments through the mucosal administration of VLPs (not shown). These data illustrate the interest to administrate locally the antigen to institute local HIV-specific immunity but also amplify the systemic immune responses.

Impact of the particulate form of the antigen

We next aimed to evaluate the impact of the particulate form of the antigen in our vaccine strategy to induce mucosal immunity. Thus, we compared in an IN/IVag prime-boost regimen (i) plasmid DNA encoding gp140 protein (HIV-DNA) primes/trimeric gp140 protein boosts with (ii) HIV-pVLP primes/HIV-VLP boosts, called “non-particulate” (protein-based) and “particulate” (VLP-based) vaccines, respectively (Figure 4A). Our results showed that both groups induced comparable T-cell responses in spleen and paLN, but the particulate vaccines elicited higher local T-cell

responses in the vaginal mucosa (Figure 4B). We also observed similar responses of IFN-γ secretion both in CD4+ and CD8+ memory T-cells (Figure S2). The quality of the induced immune responses was assessed. We noted that particulate vaccines improved the quality of T-cell immune responses since the VLP-based prime-boost strategy elicited a significant higher proportion of HIV-specific polyfunctional T cells in the vaginal mucosa, including the 3-cytokines secreting T-cells (Figure 4D).

The analysis of the humoral immune responses revealed that particulate antigens induced elevated IgG responses in sera, as well as higher IgA in vaginal washes, as compared to non-particulate antigens (Figure 4C). Moreover, the particulate vaccines elicited a more robust neutralizing response, as evidenced by the presence of neutralizing antibodies in the sera and vaginal washes of all vaccinated mice, and at higher levels compared to the non-particulate vaccines (Figure 4E). Both groups generated antibodies with cross-clade reactivity, although the levels were higher in mice immunized with particulate vaccines (Figure 4F), particularly against the C/B' clade CN54. Furthermore, the avidity index of humoral immune responses induced by particulate vaccines was significantly greater than that of non-particulate vaccines (Figure 4G) and the specificity of antibodies was different as shown by the high reactivity against the V3 loop region (Figure 4H).

Altogether, our findings emphasize the essential role of particulate antigens in triggering a "high-magnitude" of T- and B-cell responses in mucosal compartments and fostering "high-quality" immunity.

Particulate antigens enhance germinal center reaction

We next sought to investigate the mechanism by which particulate vaccines improve antibody responses following mucosal administration. A key step in development of

potent antibodies is the affinity maturation that occurs during the germinal center reaction. Thus, we aimed to examine the initial T follicular helper (Tfh) response triggered by the VLP vaccines after mucosal administration. We compared the germinal center reaction induced in mice that were immunized via IVag delivery of HIV-1 non-particulate antigens (gp140 proteins) or particulate antigens (HIV-VLPs) (Figure 5A). Firstly, we observed that VLPs were more immunogenic as the absolute numbers of paLN lymphocytes were significantly higher compared to protein group (Figure 5B). We next analysed primary follicular helper T-cell (T_{FH}) and germinal center B-cells (GCB) by flow cytometry at day 10. We observed that particulate antigens induced significantly more T_{FH} compared to non-particulate ones (Figure 5C,D). Interestingly, the T_{FH} induced after VLP immunizations were more activated than those induced by free proteins, as shown by higher level of ICOS expression (Figure 5D). These results reveal the unique property of VLPs to stimulate and activate T_{FH} cells after IVag administration. Similar conclusions were drawn when GCB were analysed (Figure 5E). Indeed, VLPs elicited significantly more GCB than gp140 trimers (Figure 5F). To note, the increase of GCB observed in the dLN of mice immunized with VLPs was perfectly correlated with the number of T_{FH} (Figure 5G) and the large size of germinal centers observed by microscopy (Figure 5H). Interestingly, upon comparing pVLPs and DNA vaccines for IN priming, we substantiated that particulate antigens triggered vigorous germinal center reactions in dLN. These reactions were characterized by higher frequencies of T_{FH} and GCB when contrasted with the response induced by plasmid DNA (Figure S4) and can be linked to increased IgG responses in both sera and BALs (Figure S4).

Particulate form of antigens for IVag boosting

The impact of particulate form of the antigen was also addressed in our mucosal prime-boost strategy by comparing the immune responses induced by particulate or non-particulate formulations upon boosting. Consequently, pVLP-primed mice were boosted with particulate (VLPs) or non-particulate (gp140 trimeric proteins) vaccines by IVag route (Figure 6A). While systemic T- and B-cell immune responses were equivalent in the two groups (Figure 6B, E), we observed significant higher IgA production and IgA-secreting B cells in genital tract (Figure 6B, C) as well as increased T-cell responses in vaginal mucosa of mice boosted with VLPs compared to proteins (Figure 6B-E). Likewise, we confirmed the importance of the particulate form of the antigen during the boost to induce both mucosal T- and B-cell responses.

Immune efficacy of the mucosal administration of particulate antigens

We assessed the quality and the effectiveness of the induced immune response through the utilization of this optimal vaccination regimen involving VLP-based particulate antigens. Thus, mice were primed twice by IN route using HIV-pVLPs and boosted twice by IVag route using HIV-VLPs (Figure 7A). An additional late IVag boost was also done at week 60 for the long-term kinetic (Figure 7A) or at week 20 (Figure 7H).

The follow-up of the antibody responses reveals that our protocol induced long-lasting memory responses. Indeed, IgG levels remained stable over a period of 3 months after vaccination and minimal decrease was observed after one year. Moreover, the antibody response can be amplified to the initial level after a delayed booster (Figure 7B). Notably, we observed that the avidity index of induced antibodies progressively increased during the prime-boost procedure, reaching 70% at W59 and then remained consistently above the 50% threshold (Figure 7C). Moreover, the late vaginal boost induced a rapid rebound of vaginal IgG and IgA, revealing the presence of long-term

specific memory B-cell and/or HIV-specific long-lived plasma cells in the mucosa (Figure S5). We also investigated the breadth of the antibody response. The epitope mapping revealed that antibodies recognizing multiple sites of HIV envelope including the V1V2 loop, CD4bs, MPER, V3 loop as well as the α4β7 region were induced (Figure 7D, S5). Moreover, we showed that the long-lasting IgG responses were cross-reacting against three different clades: clade A UG37, clade C/B' CN54 and clade D UG21 (Figure 7E). This vaccine protocol was also capable of eliciting long-term antibody activities since we detected significant neutralizing activity (Figure 7F) as well as HIV-specific ADCC (Figure 7G) at W61, which constitute a key point in HIV-vaccine development[29]. Finally, we evaluated the capacity of the vaccinated mice to inhibit in vivo the HIV transcytosis after mucosal viral challenge. Homologous HIV-pseudotyped recombinant lentivectors were administered vaginally and the viral spread was evaluated 48h later by RT-qPCR in draining lymph nodes (Figure 7H). Very interestingly, 66% of naïve mice showed viral dissemination in the dLN whereas only one mouse was positive in the vaccinated group (Figure 7I). Moreover, the absence of viral genetic material in ndLN (Figure 7I) validates our study model of HIV mucosal spreading in mice. Altogether, these results highlight the quality of the immune responses induced by our VLP-based vaccine regimen, especially in mucosa. To note, induced immunity is not mouse strain dependent, since both systemic and mucosal immune responses were observed in C57BL/6 and BALB/c mice (Figure S6). Nevertheless, some differences were noted such as the cytokine secretion patterns exhibited by memory T cells. We also observed elevated IgA levels in BALB/c mice, which may be associated with higher counts of $ICOS^+$ T_{FH} and GCB cells in comparaison to C57BL/6 (Figure S7).

Discussion

Here we confirmed the significant role of administering vaccine antigens at mucosal sites to induce mucosal T- and B-cell based immunity. We showed that targeting different mucosal sites in prime-boost strategy (IN/IVag, IN/IR) represents an interesting approach to induce both HIV-specific systemic and mucosal immune responses. The crucial importance of maintaining a balance between mucosal and systemic immunity as well as the need of humoral and cellular responses was perfectly highlighted by Khanna et al[30]. Their study revealed that exclusively inducing strict mucosal or systemic immunity is likely to be inadequate for achieving vaccine protection. They emphasized the requirement to focus on mucosal tissues capable of eliciting both systemic and local immunity[25,30–32]. We confirmed that intranasal immunization is appropriate to induce T- and B-cell specific immune responses in both systemic and mucosal compartments, including distant mucosal sites (*i.e.* vagina) that have been previously reported by others[6,22,25,33,34]. Notably, we demonstrated that there is a real interest in combining IN primes and IVag boosts since IN immunization initiates immune responses in vaginal site that can be amplified after local boost. Based on this IN/IVag immunization regimen, efficient mucosal immunity especially HIV-specific IgA-antibodies was induced in contrast to the ID/IVag vaccinal scheme. However, IN/IVag strategy was described by others as inefficient to enhance specific mucosal antibody immunity[35]. The main discrepancy with our study could be the difference of antigen formulation since we used VLPs instead of proteins. Indeed, when we compared (i) pVLP with DNA and (ii) VLP with protein, we established the critical role of the particulate nature of the antigen to induce and boost mucosal immunity. To note, immunizations were performed in absence of any adjuvants, which could potentially explain the low responses observed with the soluble proteins. More

importantly, we showed that VLPs (produced after pVLP priming or administrated as boosts) increased significantly the magnitude and the quality of T-cell responses and the level of HIV-specific antibodies in local mucosa (Figures 4, 6 and supplemental figure 4). The VLP formulation seems to be particularly appropriate for mucosal immunity induction, even in the absence of any adjuvant. The use of VLPs as potential HIV-specific vaccine candidates offers numerous advantages over traditional strategies. VLPs have the unique ability to present viral Env spikes in their natural conformation and, therefore, the potential to trigger neutralizing antibody responses against HIV[5].

Likewise, we showed that the higher HIV-specific mucosal immunity, including neutralizing and IgA antibodies, was induced after mucosal administration of VLP-based vaccines. This unique immune property of the VLPs may be also explained by an efficient germinal center response induction, as shown by high $ICOS^+$ T_{FH} and GC B cell generation and activation. Interestingly, the role of $ICOS^+$ T_{FH} for antibody response induction has been recently demonstrated in a study comparing three different priming vectors (plasmid DNA, recombinant MVA, and recombinant VSV) for HIV vaccination[36]. It was shown that the different vector-based vaccines are associated with differential development of germinal center reactivity and generation of neutralizing antibody responses but the influence of the nature of the antigens and especially its particulate form was not investigated.

Deciphering the mechanisms of VLP action on germinal center responses is still to be addressed but requires additional analysis. More generally, VLPs are described as highly immunogenic, which can be explained by their highly repetitive structure that facilitates B-cell activation due to the cross-link to the BCRs[37]. In the context of mucosal vaccination, the particulate structure of VLPs may also facilitate their passage through

the mucosal barrier and their uptake by the mucosal resident immune cells[38]. Additionally, we previously demonstrated that our VLPs activate antigen-presenting cells, thereby validating their inherent immunostimulatory properties and highlighting their potential to be used as antigenic platform[10,39]. Altogether, VLPs are promising vaccine candidates, including for mucosal vaccination. While VLP immunogenicity following mucosal vaccination has been reported before[40,41], it has been less frequently explored in the context of HIV mucosal vaccination[42–44]. Our findings presented here establish that HIV-recombinant VLPs are suitable immunogens for boosting mucosal immunity and inducing efficiently specific IgA-secreting B cells in the mucosa. Interestingly, our results showed that both IVag and IR routes of immunization could be used to boost systemic and local immunity. Nevertheless, it's now important to test the protective efficacy of the IN/IVag and the IN/IR prime-boost strategies combining HIV-pVLPs and VLPs to propose an unrestricted gender vaccine. Combinations of both IR and IVag boosts will be also assessed even if altered immune responses have been reported when different immunization routes have been associated[45].

The quality and the functionality of induced antibodies (*e.g.* transcytosis inhibition, avidity, neutralization or ADCC activity) are currently considered as critical parameters to analyse in vaccine development, since they have been correlated to HIV protection in the RV144 clinical trial[14,29,46–49]. Interestingly, the different parameters that have been correlated with protection were here collected in our study. First, we showed high Env-specific IgG and low IgA levels in sera of immunized mice, which have been associated with lower rate of infection[29,48]. Furthermore, we induced long-term systemic immunity illustrated by the stable high-avidity IgG titers over time, associated with neutralizing and ADCC activity, which are both mainly correlated with HIV protection[29,47,48,50]. A wide breadth humoral response was also observed with

antibodies targeting V1V2, V3 or the MPER region of the gp120; all of these regions especially known to be targeted by bNAbs in long-term no progressor individuals (LTNP) that control viral dissemination[51]. Additionally, our vaccine regimen induces HIV-specific polyfunctional CD4+ T-cell responses, which are also associated with protection[29,30,50].

Altogether, our results highlight the quality of the immune responses induced by our VLP-based vaccine regimen, especially in mucosa. In addition to eliciting robust systemic immune responses, we observed significant mucosal T and B cell immune responses. Notably, we detected elevated levels of vaginal SIgA antibodies, which play a crucial role in preventing HIV entry in the genital mucosa. Through an in vivo transcytosis inhibition assay, we substantiated the protective potential of our vaccine strategy, as evidenced by the lack of viral spread in mice upon subsequent challenges.

In conclusion, our study showcases the capacity of these HIV-recombinant VLP-based vaccines to effectively elicit HIV-specific, high-quality, and long-lasting immunity in both systemic and mucosal compartments following mucosal immunizations. Future studies will further evaluate this vaccination regimen using optimized antigens instead of HIV-1 native-like Env antigens and the protective efficacy in nonhuman primates after multiple intravaginal or intrarectal challenges.

Material and Methods

Cell lines

HEK293T cells (CRL-1573; ATCC) were grown in Dulbecco's modified Eagle medium (DMEM) supplemented with 2 mM L-Glutamine, 100 U/mL penicillin, 100 µg/mL

streptomycin (all from Life Technologies, Cergy Pontoise, France) and 10% heat-inactivated fetal calf serum.

Mice

6-8 weeks old female BALB/cj and C57bBL/6j mice were purchased from Janvier Labs (Le Genest-Saint-Isle, France). All the mice used for this project were female since we used intravaginal route of administration. Mice were maintained under specific pathogen-free conditions, manipulations were performed according to the EU Directive 2010/63/EU for animal experiments and approved by the local ethics committee.

Plasmids

The MLV-GagPol encoding plasmid used for VLP production and pVLP vaccination was previously described[27]. pBL211, a plasmid encoding the Gag-GFP fusion gene under the control of the human CMV promoter, was obtained from the EPX145-68 plasmid[52] by insertion of a PCR fragment with an MluI restriction site between the NruI and NheI sites. A PCR-synthesized DNA fragment encoding green fluorescent protein (GFP) with an MluI site introduced at the 5' end was then inserted at the MluI site to produce the CMV-Gag-GFP plasmid. pBL116 is a codon-optimized construct encoding the chimeric $gp140_{TM}$ envelope glycoprotein derived from HIV-1 Clade B JRFL strain. Signal peptide of the Low-Affinity Nerve Growth Factor Receptor (LNGFR) was used. The Furin site (SEKS) of gp120 was mutated to prevent its cleavage from gp41 and the TM/CT domain of gp41 was replaced by those of VSV-G. Similarly, pBL188 encodes the $gp160_{WT}$ glycoprotein in which TM/CT of gp120 is the wild-type domain.

Production of HIV-VLPs

HEK-293T were transfected using a calcium phosphate transfection protocol with MLV-Gag and HIV-$gp140_{TM}$ encoding plasmids in a 2:1 ratio and 50 µg of total DNA per 175

cm^2 flask. After 48h, supernatants were collected, filtered through 0.45µm pore-sized membranes and concentrated with Centricon (Millipore, Molsheim, France). Then, supernatants were layered on top of a sucrose step gradient (2.5 mL, 35%; 2.5 mL, 50%) and centrifuged at 100,000 g for 2h at 4°C. Interface was collected and washed with PBS in an identical step of centrifugation to eliminate remaining sucrose. VLPs were quantified by BCA (Thermo Fisher Scientific, USA) and validated by western-blot using anti-gp120, anti-gp41 (2G12 and 2F5 from Polymun Scientific GmbH, Austria) and anti-MLV-Gag antibodies (produced from hybridoma supernatants, ATCC CRL-1912 clone R187). Quantification of gp140 onto VLPs was performed by gp120-specific ELISA using the D7324 antibody from BH-10 strain (Aalto Bioreagents, Dublin, Ireland) as coating antibody and the 2G12 antibody for revelation. Gp140 quantities was determined using a standard curve with either free gp160 or $gp140_{TM}$ proteins. The pseudotyped VLPs underwent lysis using Triton 0.1% prior to conducting the ELISA. Utilizing the measurements of total protein content and that of gp120, the percentage of gp120 present on HIV-VLPs was calculated.

Immunizations

Mice previously anesthetized with a cocktail of Xylazine (10 mg/kg; Rompun 2%, Bayer Pharma, France) and Ketamine (150 mg/kg; Imalgène 1000, Merial, France) by intra-peritoneal injection were then immunized at 2 or 3 week-intervals by intranasal, intravaginal, intrarectal or intradermic routes. Intranasal injections were performed with 50 µL of plasmid DNA formulated with PEI as previously described[53]. This formulation comprised 10 µg of plasmid DNA encoding the $gp140_{TM}$ glycoprotein, in presence or not of an additional 20 µg of plasmid DNA encoding the MLV-gag core of the VLPs. Injections were performed drop by drop in one nostril. For intravaginal and intrarectal immunizations, female mice were pre-treated with 5% citric acid wad for two hours and

then injected using the MicroSprayer® Aerosolizer (PennCentury, USA) with 50 µL of 1 µg of $gp140_{TM}$ antigens (clade B, JRFL) delivered as VLPs or as soluble protein trimers (kindly provided by Dr. Richard Wyatt, USA[54]). Three days before each IVag or IR immunization, mice were synchronized with 2 mg of medroxyprogesterone (Depo-Provera, Pfizer, USA) by subcutaneous injection at the base of the tail. Intradermal immunizations were performed on shaved skin on the upper back by two injections of 25 µL each, containing equivalent quantities of plasmid DNA as the intranasal immunization. Both injection sites were then placed between two electrodes for electroporation. The skin was immediately electroporated with tweezer type electrodes (CUY650 P3 electrodes; Sonidel Limited, Dublin, Ireland) using a BTX ECM830 generator (Harvard Apparatus, Les Ulis, France). Eight pulses of 60 V were given for 20ms duration with a 200ms interval. Subcutaneous injections of VLPs were performed either with 50 µg of total VLPs or an equivalent amount of VLPs corresponding to 1 µg of $gp140_{TM}$. VLPs were diluted in 100 µL of PBS were injected at the base of the tail.

Samples collection

Sera or vaginal washes were collected before immunization or at regular intervals after the last injection. Sera were heat-inactivated at 56°C for 30 minutes. Bronchoalveolar lavages (BALs) were collected through the trachea by two series of injection-aspiration with 1 mL of PBS + 1X protease inhibitor (Protease inhibitor cocktail set I, 100X, Calbiochem, USA). Vaginal washes were collected by three repeated flushes using 40 µL of PBS and 1X protease inhibitor. After centrifugation, samples were immediately frozen at -20°C. 50-100mg of feces were crushed and homogenized in 1X protease inhibitor buffer at 100mg/ml for 1h at room temperature, before filtration and storage at -20°C. Lymph nodes were collected, and cells were prepared by digestion with Liberase TM (0.3 WU/mL; Roche Diagnostics, Meylan, France) and DNAse I (200

µg/mL; Roche Diagnostics, Meylan, France) in RPMI medium. Vaginal and rectal mucosa were removed, washed, and cut into small pieces for digestion with a cocktail of Liberase DL (0.3 WU/mL; Roche Diagnostics, Meylan, France) and DNAse I (200 µg/mL; Roche Diagnostics, Meylan, France). A 40%-80% Percoll gradient was used to isolate mucosal lymphoid cells. 50-100mg of feces were crushed and homogenized in 1X protease inhibitor buffer at 100mg/ml for 1h at room temperature, before filtration and conservation at -20°C.

Flow cytometry and antibodies

For IntraCellular Cytokine Staining (ICCS), 2 x 10^6 cells were placed on 96-well plates and restimulated or not with 50 ng/well of gp140-pseudotyped HIV-1 lentiviral vector for 16-18h at 37°C in 5% of CO_2. The last 4h, protein transport was blocked using BD Golgiplug™ (BD Biosciences, USA). Cells were then stained using protocol determined by the BD Cytofix-Cytoperm™ (BD Biosciences, USA) protocol. For immunostaining, following antibodies were used at optimal concentration: CD3-PE-CF594, CD4-V500, CD4-BV510, CD8-AF700, CD19-PE-CF594, CD44-biot, CD45-PE-CF594, CD138-PE, B220-FITC, CXCR5-biot, IL-2-FITC from BD Biosciences (USA); CD3-e450, CD95-APC, PD1-PE, IgD-PC7, GL7-e450, TNFα-PE, IFNγ-e450, ICOS-APC, Perforin–APC, Streptavidin-e780 from eBiosciences (USA). Flow cytometry was performed on the LSRII using the BD DIVA software (BD Biosciences, USA) and analyzed with Flowjo Software (Flowjo LLC, USA).

Immunofluorescent microscopy

Lymph nodes were mounted in OCT embedded compound and frozen at -80°C. 6 µm cryostat sections were performed, then fixed in 4% formaldehyde solution for 10min. After several washes, sections were permeabilized in 0.3% Triton, then blocked in BSA

1% before labelled using CD3-PE and IgD-APC (eBiosciences, USA). Acquisition were performed on inversed confocal microscope (SP2 AOBS AOTF, Leica) and analysed on ImageJ software.

ELISA

96-well microtiter plates (Nunc Life Technologies, Rochester, NY) were coated with 1 µg/mL of HIV-gp140 protein (clade B, JRFL; clade A, UG37; clade C/B', CN54 and clade D, UG21; Polymun Scientific GmbH, Austria) or pool of overlapping HIV-gp160 peptides (HIV-1 Censensus B Env peptides, Cat No. 9480, Lot No. 8 098265, NIH AIDS reagents Program, NIH, USA) at 4°C overnight. Wells were blocked with 100 µL of Superblock Blocking Buffer (Thermo Fisher Scientific, Brebières, France) for 1 h at room temperature (RT). Serial dilutions of sera, BAL, vaginal washes or feces in PBS 2% (w/v) BSA (Sigma-Aldrich) 0.1% Tween-20 (Bio-Rad Laboratories, Marnes-la-Coquette, France) were added and incubated for 2h at RT. Biotin-labeled goat anti-mouse IgG or IgA antibodies (both from CliniSciences, Montrouge, France) were added for 30 min at RT, followed by 1 hour at RT with an ultrasensitive streptavidin-peroxidase polymer (Sigma-Aldrich, USA). Plates were thoroughly washed between each step by multiple washes with PBS 0.1% Tween-20. Peroxidase activity was measured using TMB substrate (eBiosciences, USA) and optical densities were read at 450 nm (OD_{450}) after blocking the reaction by adding HCl 1N. Avidity index was evaluated using the same ELISA protocol where an additional step using sodium thiocyanate at 1.5M for 15min were performed to unbound low avidity antibodies.

Neutralization and ADCC

Neutralization assays were performed as previously described[55,56] using a standard reference strain (Clade B; SF162.LS, tier-1) to infect TZM-bl cells. Serial 3-fold dilutions

were performed starting 1/20. The 50% inhibitory dose was defined as the sample concentration that caused a 50% reduction in relative luminescence units (RLU).

ADCC was evaluated by an HIV-infected cell elimination flow-cytometry-based assay adapted from our previous protocol[57]. Briefly, CEM cells were infected using a standard reference strain of HIV-1 (Clade B; SF162.LS, tier-1: high sensitive neutralization phenotype) and infected cells were detected as p24+ cells by flow cytometry. Mouse PBMCs were used as effector cells. The effectors and target CEM cells were incubated at a 5:1 effector/target ratio in the presence or not of sera diluted at 1/20 or 1/250.

ELISPOT

Spleens, draining lymph nodes or genital mucosa cells were collected and specific IFN-γ production by T cells was determined in a standard mouse ELISPOT assay (Mabtech, Sweden). Briefly, 5 x 10^5 cells were restimulated for 48h at 37°C in 5% CO_2 with 10 µg/mL of gp140-TM peptide or 10 ng/well of $gp140_{TM}$ lentiviral particles. Medium alone and concanavalin A (ConA; Sigma-Aldrich, USA) at 3 µg/mL were used as negative and positive controls, respectively. Spots were counted with an AID ELISPOT reader (ELR03; AID, Germany). For B-cell ELISPOT, draining lymph nodes, genital or rectal mucosa were collected and total as well as gp140-specific IgG or IgA secreting B-cells were counted. Briefly, 2x10^5 cells were restimulated for 48h at 37°C in 5% CO_2 with IL-2 and R848 as recommended by the manufacturer (Mabtech, Sweden). Spots were counted with an AID ELISPOT reader (ELR03; AID, Germany). Results were expressed as spot-forming units (SFU) per 10^6 cells.

***In vivo* HIV-transcytosis inhibition assay**

Immunized mice were boosted at week 20 with HIV-VLPs, 2 weeks prior a vaginal challenge with 5 x 10^6 HIV-$gp140_{TM}$ pseudotyped lentiviral vector bearing the luciferase

reporter gene. 48 hours post-infection, para-aortic (draining, dLN) and brachial (non-draining, ndLN) lymph nodes were collected and prepared to extract whole RNA. Custom TaqMan® Gene Expression assays (Applied Biosystems, ThermoFisher) for Luc2 were designed using Primer Express® software (Applied Biosystems) ; Forward primer Luc2 : 5'CCACGCTGGGCTACTTGATC3', Reverse Primer Luc2 : 5'TCCTCCTCGAAGCGGTACAT3' and probe Luc2 : 5'CGGCTTTCGGGTCGT3'. To validate primers and probe, a ten-fold dilution series of the pGL4.10 plasmid (Promega) were used. Quantitative PCR was performed using the 7500 Fast Real-Time PCR System (Applied Biosystems, ThermoFisher) with Fast Master Mix (Applied Biosystems, ThermoFisher). The housekeeping gene used is GAPDH. The probe IDs GAPDH is Mm99999915_g1 (Applied Biosystems, ThermoFisher). qPCR was performed in triplicate and the mRNA levels were normalized with GAPDH mRNA measurements.

In vivo imaging

Anesthetized mice were IN or ID injected with 10 µg of a plasmid (pLuc) encoding the luciferase reporter enzyme either PEI-formulated or electropored, respectively. Three days later, luciferase activity was measured by i.p. administration of D-luciferin (150 mg/kg; Promega, Charbonnières-les-Bains, France) and bioluminescence images were acquired for 300 seconds maximum with the IVIS Spectrum imaging system (Caliper Life Sciences, Tremblay, France). Luciferase expression was analyzed with the Living Image 3.2 software (Caliper Life Sciences) and shown average radiance (p/s/cm²/sr). Two different PEI (InVivo JetPEI, Polyplus Transfection, France and Polyethylenimine "Max" Mw40,000, Polysciences Europe GmbH, Germany) were used and we show no difference of DNA expression between both (Figure S8).

Statistical analysis

Data are expressed as the mean ± SEM or mean ± SD when appropriate. Continuous variables were compared using the t test or Mann–Whitney U test when appropriate. All tests were two-tailed at a significance level of 0.05. Graphing and statistical analyses were performed using Prism software (GraphPad Software, USA).

Bibliography

1. Barré-Sinoussi, F. *et al.* Isolation of a T-lymphotropic retrovirus from a patient at risk for acquired immune deficiency syndrome (AIDS). *Science* 220, 868–871 (1983).
2. Rerks-Ngarm, S. *et al.* Vaccination with ALVAC and AIDSVAX to prevent HIV-1 infection in Thailand. *N. Engl. J. Med.* 361, 2209–2220 (2009).
3. Gray, G. E. *et al.* Vaccine Efficacy of ALVAC-HIV and Bivalent Subtype C gp120-MF59 in Adults. *N Engl J Med* 384, 1089–1100 (2021).
4. Vyas, S. P. & Gupta, P. N. Implication of nanoparticles/microparticles in mucosal vaccine delivery. *Expert Rev Vaccines* 6, 401–418 (2007).
5. Gao, Y., Wijewardhana, C. & Mann, J. F. S. Virus-Like Particle, Liposome, and Polymeric Particle-Based Vaccines against HIV-1. *Front. Immunol.* 9, (2018).
6. Bomsel, M. *et al.* Immunization with HIV-1 gp41 Subunit Virosomes Induces Mucosal Antibodies Protecting Nonhuman Primates against Vaginal SHIV Challenges. *Immunity* 34, 269–280 (2011).
7. Chen, C.-W., Saubi, N. & Joseph-Munné, J. Design Concepts of Virus-Like Particle-Based HIV-1 Vaccines. *Front Immunol* 11, 573157 (2020).
8. Zhang, P. *et al.* A multiclade env-gag VLP mRNA vaccine elicits tier-2 HIV-1-neutralizing antibodies and reduces the risk of heterologous SHIV infection in macaques. *Nat Med* 27, 2234–2245 (2021).
9. Tarrés-Freixas, F. *et al.* An engineered HIV-1 Gag-based VLP displaying high antigen density induces strong antibody-dependent functional immune responses. *NPJ Vaccines* 8, 51 (2023).
10. Pitoiset, F., Vazquez, T. & Bellier, B. Enveloped virus-like particle platforms: vaccines of the future? *Expert Rev Vaccines* 14, 913–915 (2015).

11. Belyakov, I. M. & Berzofsky, J. A. Immunobiology of mucosal HIV infection and the basis for development of a new generation of mucosal AIDS vaccines. *Immunity* 20, 247–253 (2004).
12. Neutra, M. R. & Kozlowski, P. A. Mucosal vaccines: the promise and the challenge. *Nat. Rev. Immunol.* 6, 148–158 (2006).
13. Belyakov, I. M. & Ahlers, J. D. What Role Does the Route of Immunization Play in the Generation of Protective Immunity against Mucosal Pathogens? *J Immunol* 183, 6883–6892 (2009).
14. Tudor, D. *et al.* HIV-1 gp41-specific monoclonal mucosal IgAs derived from highly exposed but IgG-seronegative individuals block HIV-1 epithelial transcytosis and neutralize CD4(+) cell infection: an IgA gene and functional analysis. *Mucosal Immunol* 2, 412–426 (2009).
15. Hirbod, T. *et al.* HIV-neutralizing immunoglobulin A and HIV-specific proliferation are independently associated with reduced HIV acquisition in Kenyan sex workers. *AIDS* 22, 727–735 (2008).
16. Devito, C. *et al.* Mucosal and Plasma IgA from HIV-1-Exposed Uninfected Individuals Inhibit HIV-1 Transcytosis Across Human Epithelial Cells. *J Immunol* 165, 5170–5176 (2000).
17. Belyakov, I. M. & Ahlers, J. D. Mucosal immunity and HIV-1 infection: applications for mucosal AIDS vaccine development. *Curr. Top. Microbiol. Immunol.* 354, 157–179 (2012).
18. Wijesundara, D. K., Ranasinghe, C., Grubor-Bauk, B. & Gowans, E. J. Emerging Targets for Developing T Cell-Mediated Vaccines for Human Immunodeficiency Virus (HIV)-1. *Front Microbiol* 8, 2091 (2017).
19. Donnelly, L. *et al.* Intravaginal immunization using the recombinant HIV-1 clade-C trimeric envelope glycoprotein CN54gp140 formulated within lyophilized solid dosage forms. *Vaccine* 29, 4512–4520 (2011).
20. McKay, P. F. *et al.* Intravaginal immunisation using a novel antigen-releasing ring device elicits robust vaccine antigen-specific systemic and mucosal humoral immune responses. *J Control Release* 249, 74–83 (2017).
21. Wang, S.-W. *et al.* An SHIV DNA/MVA rectal vaccination in macaques provides systemic and mucosal virus-specific responses and protection against AIDS. *AIDS Res. Hum. Retroviruses* 20, 846–859 (2004).

22. Johansson, E.-L., Wassén, L., Holmgren, J., Jertborn, M. & Rudin, A. Nasal and Vaginal Vaccinations Have Differential Effects on Antibody Responses in Vaginal and Cervical Secretions in Humans. *Infect. Immun.* 69, 7481–7486 (2001).
23. Sato, A. *et al.* Vaginal memory T cells induced by intranasal vaccination are critical for protective T cell recruitment and prevention of genital HSV-2 disease. *J. Virol.* 88, 13699–13708 (2014).
24. Wern, J. E., Sorensen, M. R., Olsen, A. W., Andersen, P. & Follmann, F. Simultaneous Subcutaneous and Intranasal Administration of a CAF01-Adjuvanted Chlamydia Vaccine Elicits Elevated IgA and Protective Th1/Th17 Responses in the Genital Tract. *Front Immunol* 8, 569 (2017).
25. Hartwell, B. L. *et al.* Intranasal vaccination with lipid-conjugated immunogens promotes antigen transmucosal uptake to drive mucosal and systemic immunity. *Sci Transl Med* 14, eabn1413 (2022).
26. Huret, C. *et al.* Recombinant retrovirus-derived virus-like particle-based vaccines induce hepatitis C virus-specific cellular and neutralizing immune responses in mice. *Vaccine* 31, 1540–1547 (2013).
27. Bellier, B. *et al.* DNA vaccines encoding retrovirus-based virus-like particles induce efficient immune responses without adjuvant. *Vaccine* 24, 2643–2655 (2006).
28. Bellier, B. *et al.* DNA vaccines expressing retrovirus-like particles are efficient immunogens to induce neutralizing antibodies. *Vaccine* 27, 5772–5780 (2009).
29. Haynes, B. F. *et al.* Immune-correlates analysis of an HIV-1 vaccine efficacy trial. *N. Engl. J. Med.* 366, 1275–1286 (2012).
30. Khanna, M. *et al.* Mucosal and systemic SIV-specific cytotoxic CD4 + T cell hierarchy in protection following intranasal/intramuscular recombinant pox-viral vaccination of pigtail macaques. *Scientific Reports* 9, 1–16 (2019).
31. Tomusange, K. *et al.* Mucosal vaccination with a live recombinant rhinovirus followed by intradermal DNA administration elicits potent and protective HIV-specific immune responses. *Sci Rep* 6, 36658 (2016).
32. Jensen, K. *et al.* Vaccine-Elicited Mucosal and Systemic Antibody Responses Are Associated with Reduced Simian Immunodeficiency Viremia in Infant Rhesus Macaques. *J. Virol.* 90, 7285–7302 (2016).
33. Rudin, A., Johansson, E.-L., Bergquist, C. & Holmgren, J. Differential Kinetics and Distribution of Antibodies in Serum and Nasal and Vaginal Secretions after Nasal and Oral Vaccination of Humans. *Infect. Immun.* 66, 3390–3396 (1998).

34. Xiao, P. *et al.* Parainfluenza Virus 5 Priming Followed by SIV/HIV Virus-Like-Particle Boosting Induces Potent and Durable Immune Responses in Nonhuman Primates. *Front Immunol* 12, 623996 (2021).
35. Tregoning, J. S. *et al.* A 'prime-pull' vaccine strategy has a modest effect on local and systemic antibody responses to HIV gp140 in mice. *PLoS ONE* 8, e80559 (2013).
36. Eslamizar, L. *et al.* Recombinant MVA-prime elicits neutralizing antibody responses by inducing antigen-specific B cells in the germinal center. *NPJ Vaccines* 6, 15 (2021).
37. Spohn, G. & Bachmann, M. F. Exploiting viral properties for the rational design of modern vaccines. *Expert Rev Vaccines* 7, 43–54 (2008).
38. Schneider-Ohrum, K. & Ross, T. M. Virus-like particles for antigen delivery at mucosal surfaces. *Curr. Top. Microbiol. Immunol.* 354, 53–73 (2012).
39. Pitoiset, F. *et al.* Retrovirus-Based Virus-Like Particle Immunogenicity and Its Modulation by Toll-Like Receptor Activation. *J. Virol.* 91, (2017).
40. LoBue, A. D., Thompson, J. M., Lindesmith, L., Johnston, R. E. & Baric, R. S. Alphavirus-adjuvanted norovirus-like particle vaccines: heterologous, humoral, and mucosal immune responses protect against murine norovirus challenge. *J. Virol.* 83, 3212–3227 (2009).
41. Liu, X. S., Abdul-Jabbar, I., Qi, Y. M., Frazer, I. H. & Zhou, J. Mucosal immunisation with papillomavirus virus-like particles elicits systemic and mucosal immunity in mice. *Virology* 252, 39–45 (1998).
42. Buonaguro, L. *et al.* DNA-VLP prime-boost intra-nasal immunization induces cellular and humoral anti-HIV-1 systemic and mucosal immunity with cross-clade neutralizing activity. *Vaccine* 25, 5968–5977 (2007).
43. Sun, X. *et al.* Membrane-anchored CCL20 augments HIV Env-specific mucosal immune responses. *Virol J* 14, 163 (2017).
44. Vassilieva, E. V. *et al.* Enhanced mucosal immune responses to HIV virus-like particles containing a membrane-anchored adjuvant. *mBio* 2, e00328-00310 (2011).
45. Mann, J. F. S. *et al.* Mucosal application of gp140 encoding DNA polyplexes to different tissues results in altered immunological outcomes in mice. *PLoS ONE* 8, e67412 (2013).

46. Pegu, P. *et al.* Antibodies with High Avidity to the gp120 Envelope Protein in Protection from Simian Immunodeficiency Virus SIVmac251 Acquisition in an Immunization Regimen That Mimics the RV-144 Thai Trial. *J. Virol.* 87, 1708–1719 (2013).
47. Pegu, A. *et al.* Neutralizing antibodies to HIV-1 envelope protect more effectively in vivo than those to the CD4 receptor. *Sci Transl Med* 6, 243ra88 (2014).
48. Tomaras, G. D. *et al.* Vaccine-induced plasma IgA specific for the C1 region of the HIV-1 envelope blocks binding and effector function of IgG. *Proc. Natl. Acad. Sci. U.S.A.* 110, 9019–9024 (2013).
49. Zolla-Pazner, S. *et al.* Analysis of V2 Antibody Responses Induced in Vaccinees in the ALVAC/AIDSVAX HIV-1 Vaccine Efficacy Trial. *PLoS ONE* 8, e53629 (2013).
50. Souza, M. S. de *et al.* The Thai Phase III Trial (RV144) Vaccine Regimen Induces T Cell Responses That Preferentially Target Epitopes within the V2 Region of HIV-1 Envelope. *J Immunol* 188, 5166–5176 (2012).
51. González, N. *et al.* Characterization of broadly neutralizing antibody responses to HIV-1 in a cohort of long term non-progressors. *PLoS ONE* 13, e0193773 (2018).
52. Garrone, P. *et al.* A Prime-Boost Strategy Using Virus-Like Particles Pseudotyped for HCV Proteins Triggers Broadly Neutralizing Antibodies in Macaques. *Sci Transl Med* 3, 94ra71-94ra71 (2011).
53. Torrieri-Dramard, L. *et al.* Intranasal DNA vaccination induces potent mucosal and systemic immune responses and cross-protective immunity against influenza viruses. *Mol. Ther.* 19, 602–611 (2011).
54. Chakrabarti, B. K. *et al.* Robust Neutralizing Antibodies Elicited by HIV-1 JRFL Envelope Glycoprotein Trimers in Nonhuman Primates. *J. Virol.* 87, 13239–13251 (2013).
55. Mascola, J. R. *et al.* Recommendations for the Design and Use of Standard Virus Panels To Assess Neutralizing Antibody Responses Elicited by Candidate Human Immunodeficiency Virus Type 1 Vaccines. *J. Virol.* 79, 10103–10107 (2005).
56. Li, M. *et al.* Human Immunodeficiency Virus Type 1 env Clones from Acute and Early Subtype B Infections for Standardized Assessments of Vaccine-Elicited Neutralizing Antibodies. *J. Virol.* 79, 10108–10125 (2005).
57. Mayr, L. M. *et al.* Non-neutralizing Antibodies Targeting the V1V2 Domain of HIV Exhibit Strong Antibody-Dependent Cell-mediated Cytotoxic Activity. *Sci Rep* 7, 12655 (2017).

Acknowledgments

This project was part of the European Commission funding CUT'HIVAC from the FP7-HEALTH (Grant agreement ID: 241904) coordinated by Dr Béhazine Combadière. We thank the animal facility CEF UMS28 for all the help provided in this project and Dr Combadière for the opportunity to participate to CUT'HIVAC.

Author Contributions

T.V. and B.Be. designed experiments. T.V., L.T-D., F.P., B.L., J.V., L.M., F.B. and B.Bo. performed the experiments. T.V., D.K. and B.Be interpreted results. T.V and B.Be wrote the manuscript. B.Be conceptualized and supervised the project.

Figure 1

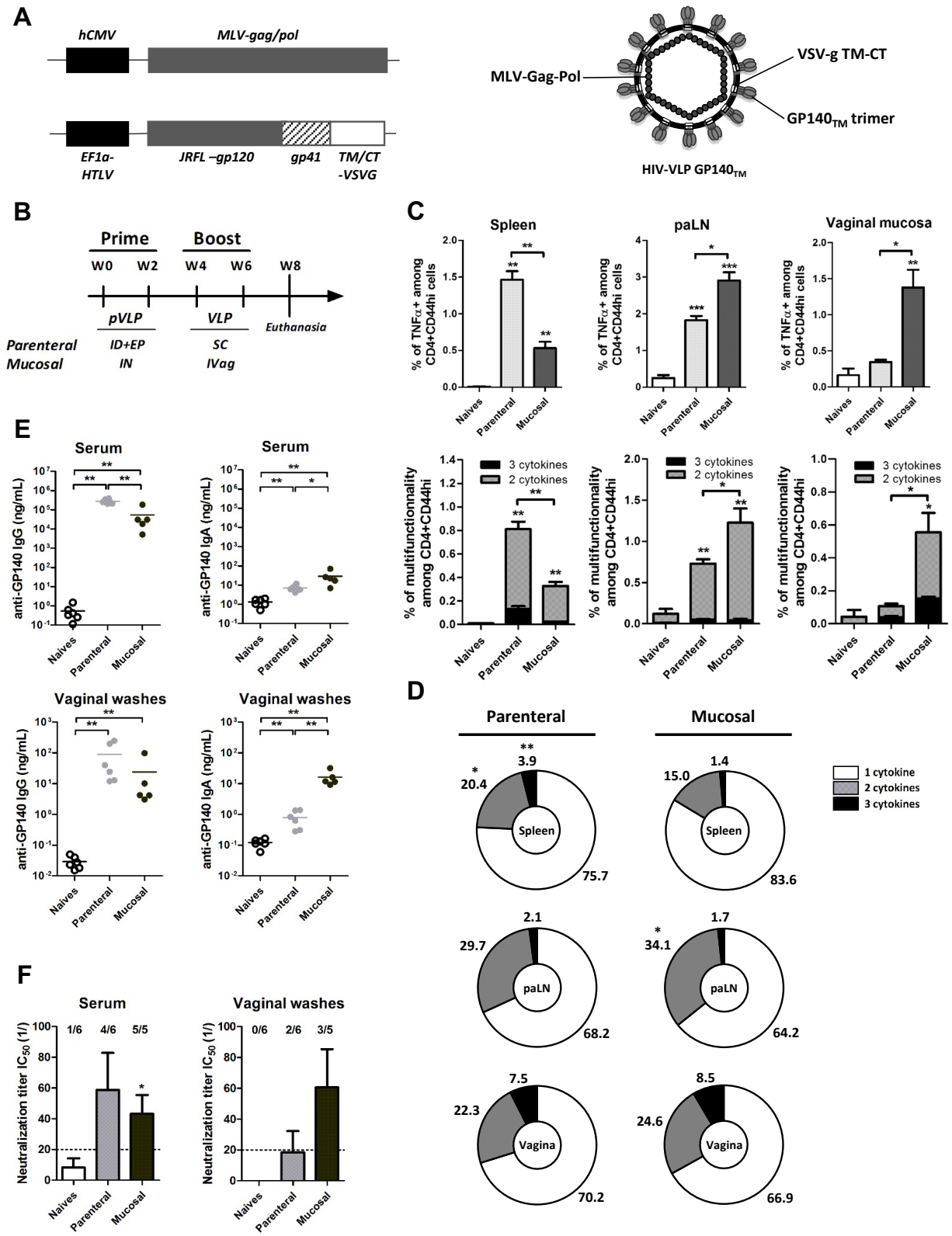
A
hCMV
MLV-gag/pol
EF1a-HTLV
JRFL –gp120
gp41
TM/CT -VSVG
MLV-Gag-Pol
VSV-g TM-CT
GP140TM trimer
HIV-VLP GP140TM
B
Prime
Boost
W0
W2
W4
W6
W8
pVLP
VLP
Euthanasia
Parenteral
ID+EP
SC
Mucosal
IN
IVag
C
Spleen
paLN
Vaginal mucosa
% of TNFα+ among CD4+CD44hi cells
% of multifunctionnality among CD4+CD44hi
3 cytokines
2 cytokines
Naives
Parenteral
Mucosal
D
Parenteral
Mucosal
1 cytokine
2 cytokines
3 cytokines
Spleen
paLN
Vagina
E
Serum
Vaginal washes
anti-GP140 IgG (ng/mL)
anti-GP140 IgA (ng/mL)
F
Neutralization titer IC50 (1/)
1/6
4/6
5/5
0/6
2/6
3/5

Figure 2

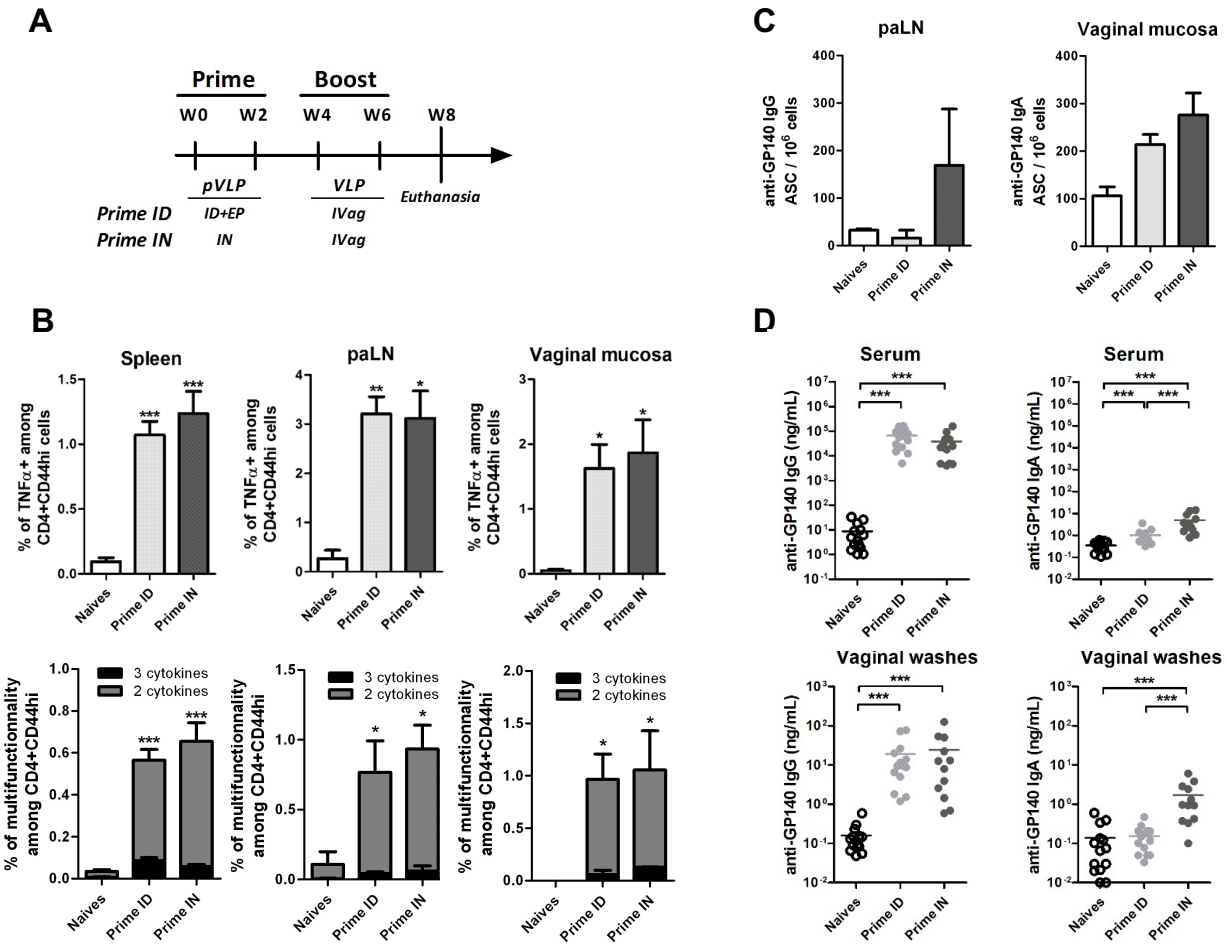
A
Prime
Boost
W0
W2
W4
W6
W8
pVLP
VLP
Euthanasia
Prime ID
ID+EP
IVag
Prime IN
IN
IVag
B
Spleen
paLN
Vaginal mucosa
% of TNFα+ among CD4+CD44hi cells
% of multifunctionnality among CD4+CD44hi
3 cytokines
2 cytokines
Naives
Prime ID
Prime IN
C
paLN
Vaginal mucosa
anti-GP140 IgG ASC / 10^6 cells
anti-GP140 IgA ASC / 10^6 cells
D
Serum
Vaginal washes
anti-GP140 IgG (ng/mL)
anti-GP140 IgA (ng/mL)

Figure 3

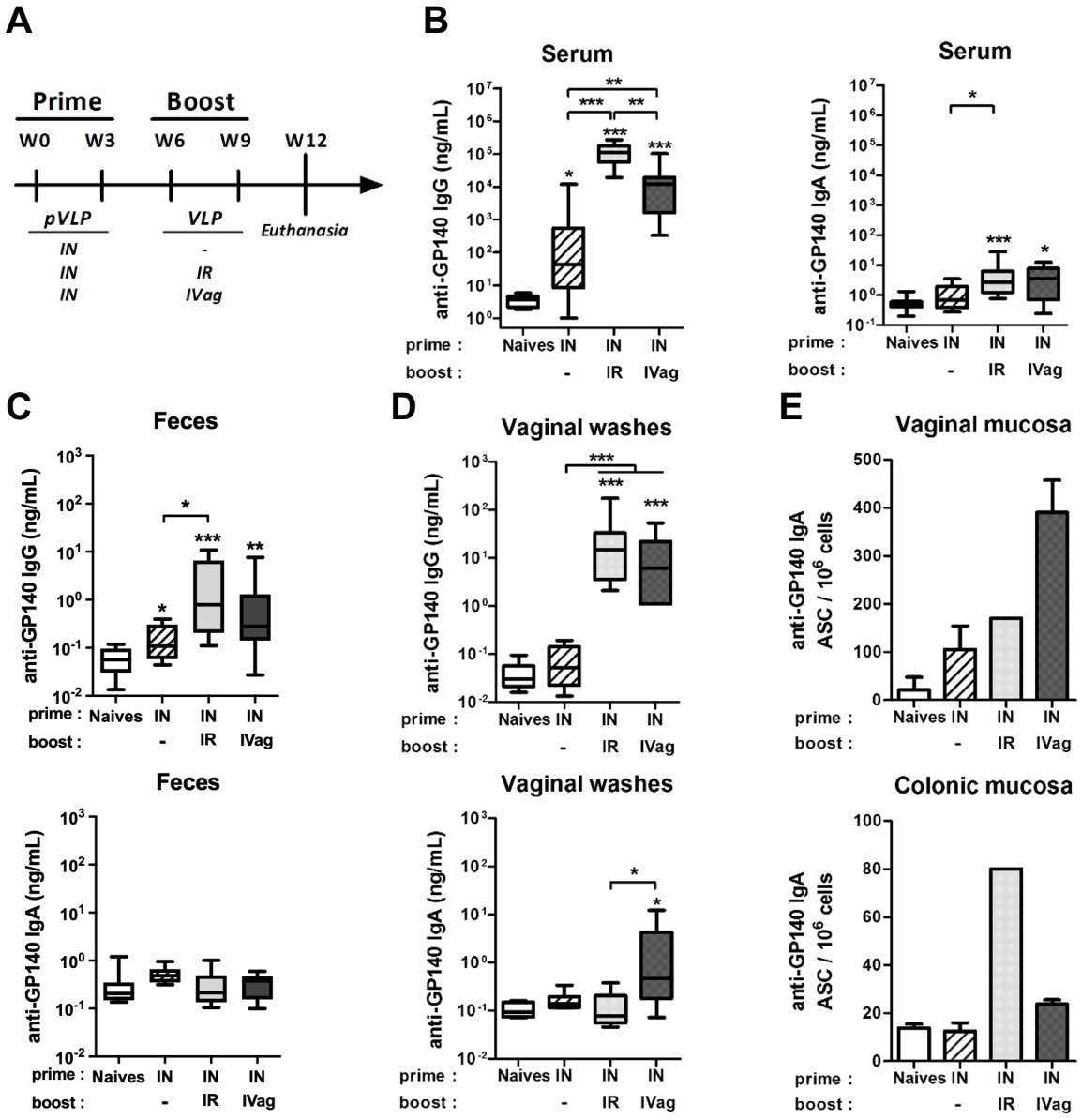
A
Prime
Boost
W0
W3
W6
W9
W12
pVLP
VLP
Euthanasia
IN
IN
IN
-
IR
IVag
B
Serum
anti-GP140 IgG (ng/mL)
anti-GP140 IgA (ng/mL)
prime :
boost :
Naives
IN
IN
IN
-
IR
IVag
C
Feces
anti-GP140 IgG (ng/mL)
anti-GP140 IgA (ng/mL)
D
Vaginal washes
E
Vaginal mucosa
anti-GP140 IgA ASC / 10^6 cells
Colonic mucosa

Figure 4

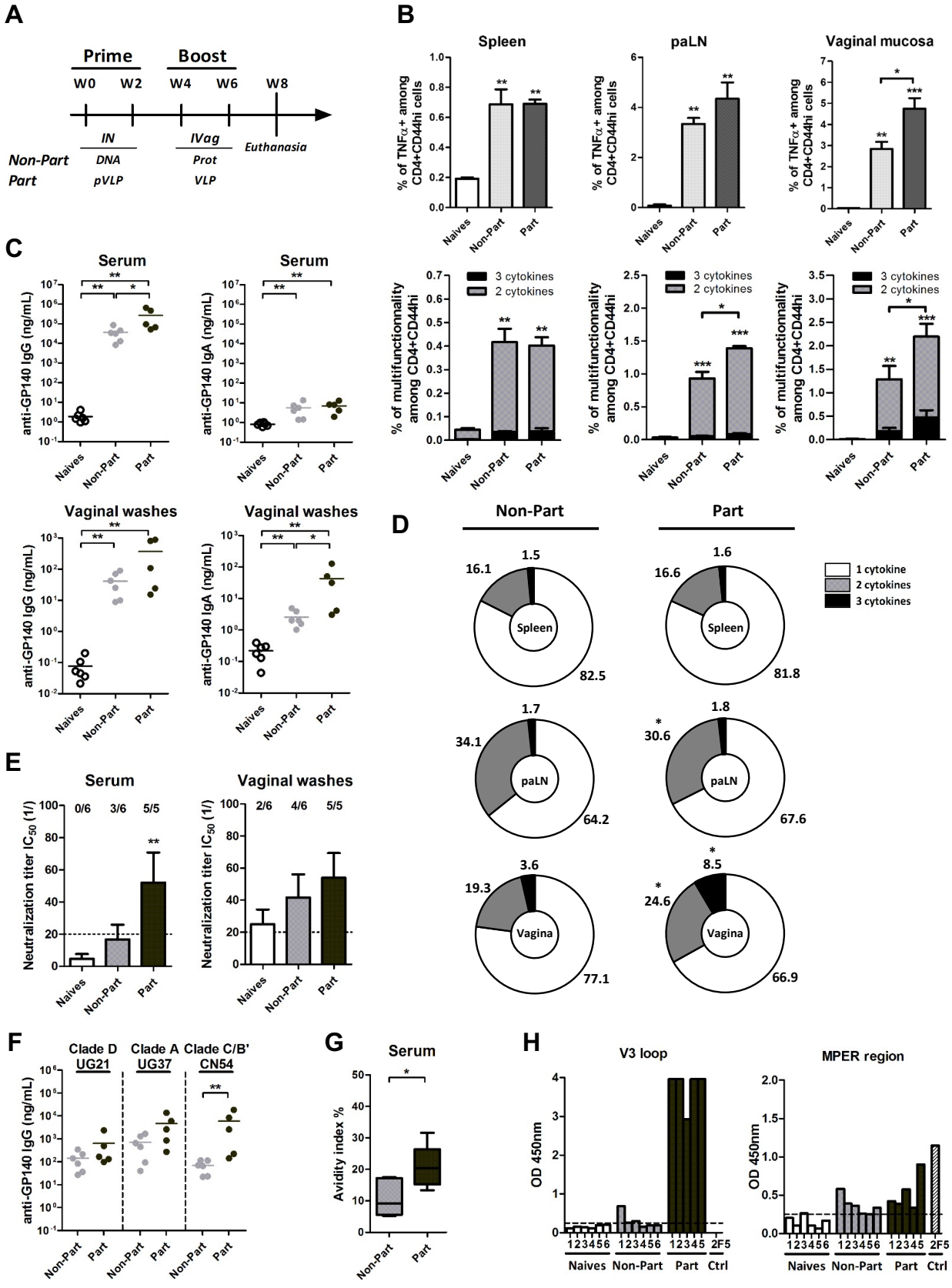
A
Prime
Boost
W0
W2
W4
W6
W8
IN
IVag
Euthanasia
Non-Part
DNA
Prot
Part
pVLP
VLP
B
Spleen
paLN
Vaginal mucosa
% of TNFα+ among CD4+CD44hi cells
3 cytokines
2 cytokines
% of multifunctionnality among CD4+CD44hi
Naives
Non-Part
Part
C
Serum
anti-GP140 IgG (ng/mL)
anti-GP140 IgA (ng/mL)
Vaginal washes
D
Non-Part
Part
1 cytokine
2 cytokines
3 cytokines
Spleen
paLN
Vagina
E
Neutralization titer IC50 (1/)
0/6
3/6
5/5
2/6
4/6
5/5
F
Clade D UG21
Clade A UG37
Clade C/B' CN54
G
Avidity index %
H
V3 loop
MPER region
OD 450nm
Naives
Non-Part
Part
Ctrl

Figure 5

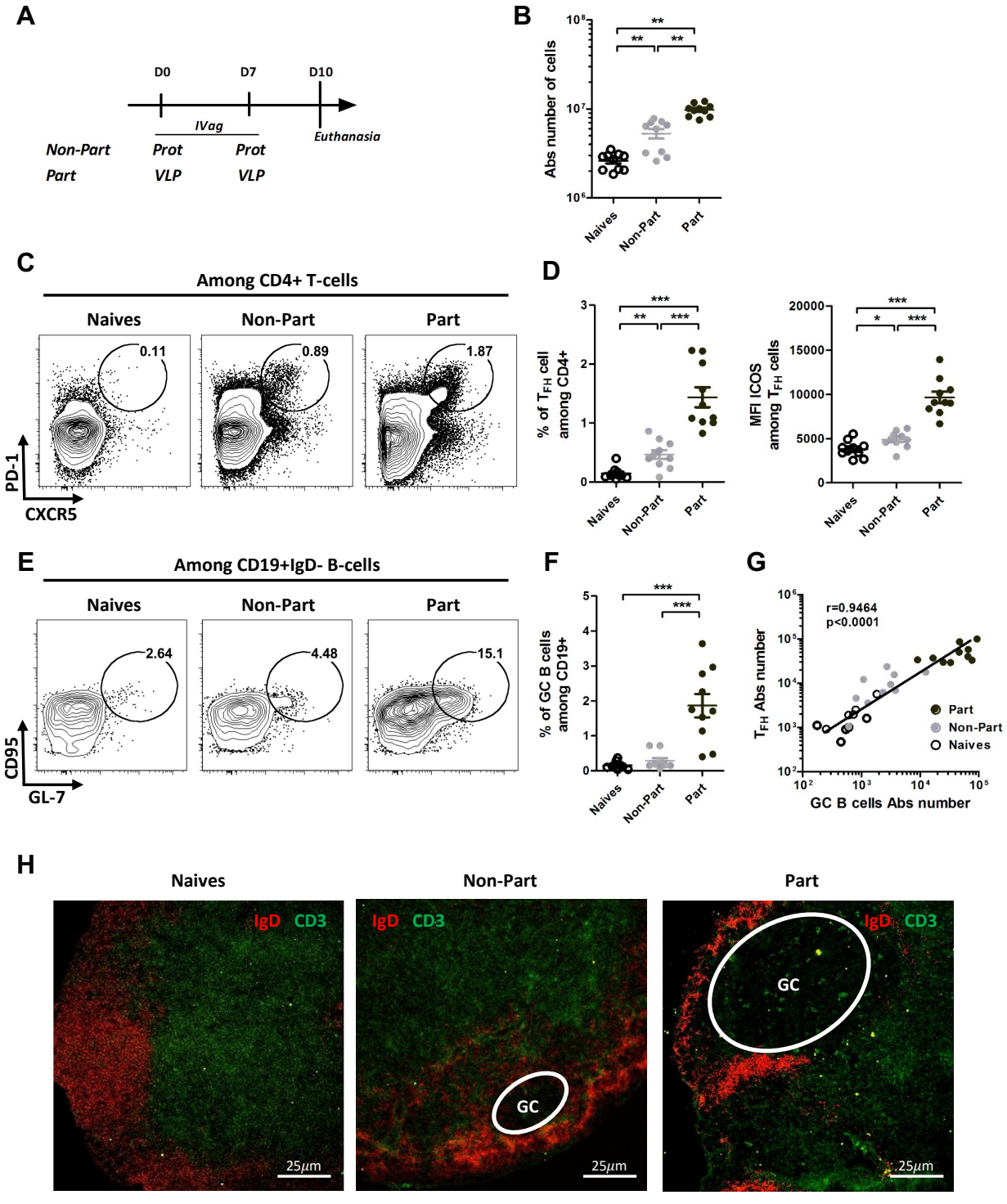
A
D0
D7
D10
IVag
Euthanasia
Non-Part
Part
Prot
VLP
Prot
VLP
B
Abs number of cells
Naives
Non-Part
Part
C
Among CD4+ T-cells
Naives
Non-Part
Part
0.11
0.89
1.87
PD-1
CXCR5
D
% of TFH cell among CD4+
MFI ICOS among TFH cells
E
Among CD19+IgD- B-cells
2.64
4.48
15.1
CD95
GL-7
F
% of GC B cells among CD19+
G
r=0.9464
p<0.0001
TFH Abs number
GC B cells Abs number
Part
Non-Part
Naives
H
IgD CD3
GC
25µm

Figure 6

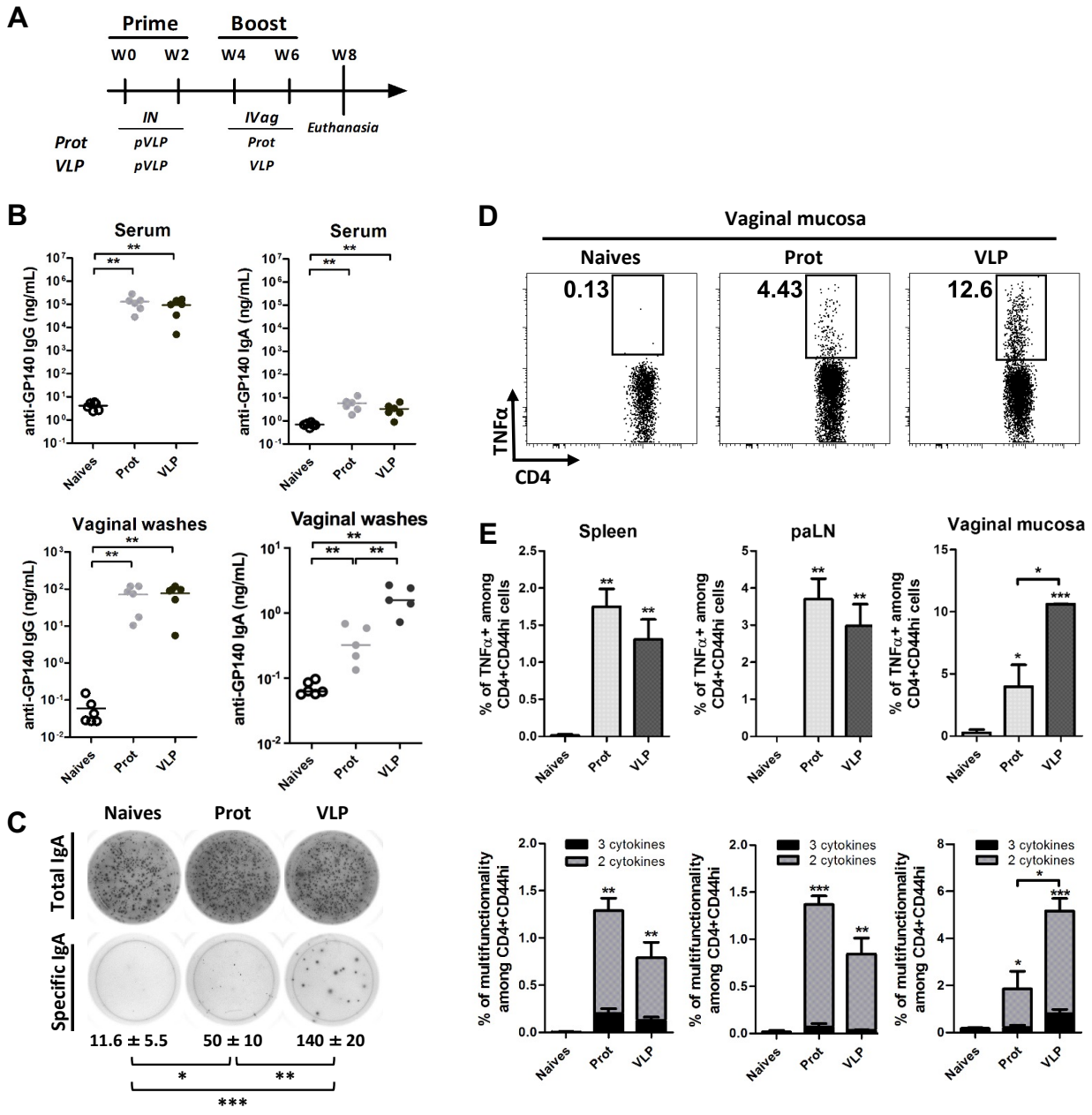
A
Prime
Boost
W0
W2
W4
W6
W8
IN
IVag
Euthanasia
Prot
pVLP
Prot
VLP
pVLP
VLP
B
Serum
anti-GP140 IgG (ng/mL)
anti-GP140 IgA (ng/mL)
Vaginal washes
Naives
Prot
VLP
C
Naives
Prot
VLP
Total IgA
Specific IgA
11.6 ± 5.5
50 ± 10
140 ± 20
D
Vaginal mucosa
0.13
4.43
12.6
TNFα
CD4
E
Spleen
paLN
Vaginal mucosa
% of TNFα+ among CD4+CD44hi cells
% of multifunctionnality among CD4+CD44hi
3 cytokines
2 cytokines

Figure 7

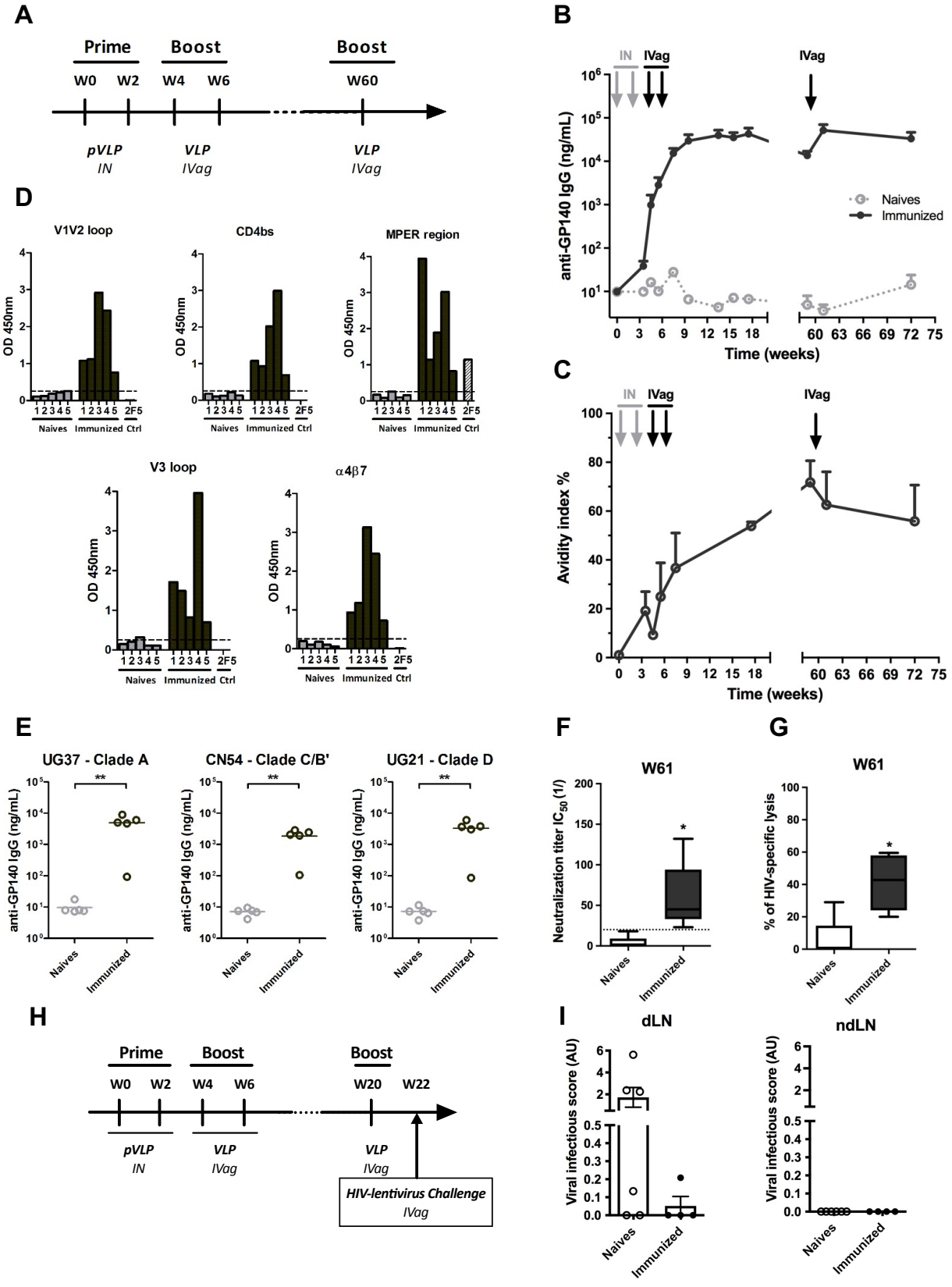
A
Prime
Boost
Boost
W0
W2
W4
W6
W60
pVLP
IN
VLP
IVag
VLP
IVag
B
IN
IVag
IVag
anti-GP140 IgG (ng/mL)
Naives
Immunized
Time (weeks)
C
IN
IVag
IVag
Avidity index %
Time (weeks)
D
V1V2 loop
CD4bs
MPER region
V3 loop
α4β7
OD 450nm
Naives
Immunized
Ctrl
2F5
E
UG37 - Clade A
CN54 - Clade C/B'
UG21 - Clade D
anti-GP140 IgG (ng/mL)
Naives
Immunized
F
W61
Neutralization titer IC50 (1/)
G
W61
% of HIV-specific lysis
H
Prime
Boost
Boost
W0
W2
W4
W6
W20
W22
pVLP
IN
VLP
IVag
VLP
IVag
HIV-lentivirus Challenge
IVag
I
dLN
ndLN
Viral infectious score (AU)
Naives
Immunized

Figure Legends

Figure 1: Influence of the immunization routes on systemic and mucosal immune responses in pVLP/VLP prime-boost strategy. (A) Schematic representation of HIV-pVLP (left) and HIV-VLP (right) vaccines. (B) Immunization protocol. BALB/c mice (n=6 per group) were immunized twice at two-week interval with HIV-pVLPs (30 µg of total DNA per mouse) by ID+EP or IN route of immunizations, then boosted twice with HIV-VLPs (1 µg of $gp140_{TM}$ per mouse) by SC or IVag routes respectively. HIV-specific T- and B-cell immune responses were analysed two weeks after the last immunization. (C) HIV-specific T-cell immune responses. TNFα-secreting T cells were monitored by intracellular cytokine staining (ICCS) after specific restimulation of cells from spleen, para-aortic lymph nodes (paLN) and vaginal mucosa. The percentage of polyfunctional T cells was determined based on the IFN-γ, TNF-α and IL-2 secretions. (D) Polyfunctionality indexes were measured among cytokine-secreting T-cells (C) and reveal the proportion of 1-, 2- and 3-cytokines secreting T-cells among total secreting cells. (E) Concentrations of IgG and IgA antibodies were measured in serum and vaginal washes by gp120-specific ELISA. (F) Neutralizing antibodies. IC50 neutralizing activity were measured in serum and vaginal washes of immunized and control mice. Numbers indicate the proportion of responding animals with a neutralization activity higher than 1/20 (positivity threshold). Data represent two independent experiments. *, $p<0.05$; **, $p<0.01$; ***, $p<0.001$; Mann-Whitney, compared to controls or between the two indicated groups (n= 5 to 6).

Figure 2: Importance of intranasal priming to induce mucosal IgA responses in pVLP/VLP prime-boost strategy.

(A) Immunization protocol. BALB/c mice (n=6 per group) were immunized twice at two-week interval with HIV-pVLPs (30 µg of total DNA per mouse) by ID+EP or IN route of immunization, then boosted twice with HIV-VLPs (1 µg of $gp140_{TM}$ per mouse) by IVag route. (B) HIV-specific memory T cell immune responses. TNFα-secreting T cells were determined by ICCS after specific restimulation in spleen, paLN and vaginal mucosa. The percentage of polyfunctional T cells was determined based on the IFN-γ, TNFα and IL-2 secretions. (C) HIV-specific IgG-secreting B-cells and IgA-specific secreting B-cells were evaluated by B-cell ELISPOT in paLN and vaginal mucosa, respectively. (D) Concentrations of IgG- and IgA- antibodies were measured in serum and vaginal washes by ELISA. Data represent pooled results of two different experiments (n=12). *, $p<0.05$; **, $p<0.01$; ***, $p<0.001$, Mann-Whitney, compared to controls or between the two indicated groups.

Figure 3: Influence of intrarectal or intravaginal delivery of VLP boost in prime-boost strategy. (A) Immunization protocol. BALB/c mice (n=8 per group) were immunized at three-week intervals by two primes with HIV-pVLPs (30 µg of total DNA per mouse) injected intranasally and two boosts with HIV-VLPs (1 µg of $gp140_{TM}$ per mouse), injected either by intravaginal or intrarectal route. HIV-specific T- and B-cell immune responses were analysed three weeks after the last immunization. Anti-gp140 specific IgG and IgA concentrations were evaluated by ELISA in sera (B), feces (C) and vaginal washes (D). (E) Specific IgA-secreting B cells were quantified by B-cell ELISPOT in colonic and vaginal mucosa (2 pools of 4 mice per group). *, $p<0.05$; **, $p<0.01$; ***, $p<0.001$; Mann-Whitney, compared to controls or between the two indicated groups.

Figure 4: Influence of the particulate form of the antigen on systemic and mucosal immunity in prime-boost strategy. (A) Immunization protocol. BALB/c mice

(n=6 per group) were immunized twice at two-week interval by intranasal injection (IN) either with gp140-DNA or HIV-pVLPs (10 µg or 30 µg respectively of total DNA per mouse) and then boosted twice by intravaginal immunizations with gp140 recombinant proteins or HIV-VLPs respectively (1 µg of $gp140_{TM}$ per mouse). (B) HIV-specific systemic and mucosal memory T-cell immune responses. TNFα-secreting T cells were monitored by ICCS after specific antigen restimulation of cells from spleen, paLN and vaginal mucosa. The percentage of polyfunctional T cells was determined based on the IFN-γ, TNFα and IL-2 secretions and polyfunctionality indexes (D) were measured among cytokine-secreting T-cells revealing the proportion of 1-, 2- and 3-cytokines secreting T-cells among total secreting cells. (C) Concentrations of IgG and IgA antibodies were measured in serum and vaginal washes by ELISA. (E) Neutralizing antibodies. IC50 neutralizing activity were measured in serum and vaginal washes of immunized and control mice. Numbers indicate the proportion of responding animals with a neutralization activity higher than 1/20 (positivity threshold). (F) Cross-clade reactivities of elicited antibodies were evaluated against three different viral strain: UG37 (clade A), CN54 (clade C/B') and UG21 (clade D). (G) Avidity index was evaluated at the end of the protocol using ELISA with sodium thiocyanate. (H) Breadth of the antibody response was evaluated by an epitope mapping assay using HIV-gp140 specific linear overlapping peptides. Specific responses against V3 loop and MPER region were represented. As controls, MPER-specific mAb (2F5) were used. Data represent two independent experiments. *, $p<0.05$; **, $p<0.01$; ***, $p<0.001$; Mann-Whitney, compared to controls or between the two indicated groups (n= 5 to 6).

Figure 5: Influence of the particulate form of the antigen on T_{FH} and germinal center responses after IVag delivery. (A) Immunization protocol. BALB/c mice (n=5 per group) were immunized twice at days 0 and 7 by IVag route with gp140

recombinant protein or HIV-VLPs (1 µg of $gp140_{TM}$ per mouse). Germinal center reactions were analyzed at day 10 in paLN. (B) Absolute cell numbers of paLN in immunized and control mice. (C-D) T_{FH} immune response. (C) Dot plots representing CXCR5+PD1+ follicular T cells among CD4+ T cells. (D) % of T_{FH} cells characterized as CD4+CXCR5+PD1+FoxP3-Bcl6+ among CD4+ T cells and activation state illustrated by ICOS MFI in T_{FH}. (E) Dot plots representing CD95+GL7+ GCB among CD19+IgD- B cells. (F) % of GCB characterized as CD19+IA/E+IgD-CD95+GL7+ among CD19+ B cells. (G) Linear correlation between T_{FH} and GCB absolute numbers in immunized and control mice. (H) Immunofluorescence microscopy. paLN sections of immunized and control mice were stained with anti-CD3-FITC and anti-IgD-APC to detect T cell zones (green) and B cell zones (red), respectively. Germinal center (GC) were characterized as areas with a loss of the IgD staining in the B cell zone. (B-D) Data represent pooled results of two independent experiments. *, $p<0.05$; **, $p<0.01$; ***, $p<0.001$, Mann-Whitney, compared to controls or between the two indicated groups (n=10).

Figure 6: Influence of the particulate form of the antigen for intravaginal boosting in prime-boost strategy. (A) Immunization protocol. BALB/c mice (n=6 per group) were primed twice at two-week intervals with HIV-pVLPs (30 µg of total DNA per mouse) by intranasal route and then boosted twice at two-week intervals either with gp140 proteins or HIV-VLPs (1 µg of $gp140_{TM}$ per mouse) by IVag route of immunization. (B) HIV-specific systemic and mucosal B cell immune responses. Concentrations of HIV-specific IgG and IgA antibodies were measured by gp140-specific ELISA in serum and vaginal washes. (C) Total and HIV-specific IgA-secreting B cells were detected by B cell ELISPOT in the vaginal mucosa. (D-E) HIV-specific T-cell memory immune responses. TNFα- secreting T cells were determined by ICCS

after antigen restimulation in spleen, paLN and vaginal mucosa. The percentage of polyfunctional T cells was determined based on the IFN-γ, TNFα and IL-2 secretions (bottom panels). (*, $p<0.05$; **, $p<0.01$; ***, $p<0.001$; Mann-Whitney, compared to controls or between the two indicated groups (n= 5 to 6); Data represent two independent experiments)

Figure 7: Mucosal prime-boost using particulate forms of the antigen induced long-lasting and high quality antibody immune responses. (A) Immunization protocol. BALB/c mice (n=5 per group) were primed two times at two-week intervals with HIV-pVLPs (30 µg of total DNA per mouse) by intranasal route and then boosted twice at two-week intervals with HIV-VLPs (1 µg of $gp140_{TM}$ per mouse) by intravaginal route. At W60, mice were additionally boosted with HIV-VLPs (1 µg of $gp140_{TM}$ per mouse) by intravaginal route. (B) HIV-specific IgG antibody response in serum was determined by ELISA over a period of 72 weeks. (C) Avidity index was evaluated over the same period of time. (D) Breadth of the antibody response was evaluated by an epitope mapping assay using HIV-gp140 specific linear overlapping peptides. Specific responses against V1V2 loop, CD4bs, MPER region, V3 loop and α4β7bs were represented at week 61. As controls, MPER-specific mAb (2F5) were used. (E) Cross-clade reactivities of elicited antibodies were evaluated against three different viral strain: UG37 (clade A), CN54 (clade C/B') and UG21 (clade D). Cross-clade response were represented at week 61. (F) Neutralizing antibodies. IC50 neutralizing activity were measured against SF162 Tier-1 HIV strain (G) ADCC activity. HIV-specific lysis of infected CEMR5 target cells was measured after incubation with serum (diluted 1:20) of immunized or naïve mice in presence of mouse effector splenocytes. (*, $p<0.05$; **, $p<0.01$; ***, $p<0.001$; Mann-Whitney, compared to naïves). (H) in vivo HIV transcytosis inhibition. 5.10^6 lentiviral particles were administered by intravaginal inoculation 48h

after a late VLP boost at week 20. (I) Viral infection score in dLN and ndLN of naives or vaccinated mice. The score illustrated an inverse correlation with the HIV transcytosis inhibition.

Supplemental figures legends and figures

Figure S1: Validation of HIV-VLPs. (A) Western-blot analysis of gp160- and $gp140_{TM}$-pseudotyped VLPs revealed with anti-gp120, anti-gp41 (left panel) and anti-MLV-Gag specific antibodies (right panel). (B) Quantification of envelope glycoproteins onto VLPs. Envelope glycoprotein concentrations were measured in gp160- and $gp140_{TM}$-pseudotyped VLPs with gp120-specific ELISA using a standard curve with either free gp160 or $gp140_{TM}$ proteins (left panel; n=3; ***, $p<0.001$, Unpaired t-test) Pseudotyped VLPs were lysed using Triton 0,1% before ELISA. Based on the total protein quantities and those of gp120, % of gp120 onto HIV-VLPs were determined. (C) Validation of natural conformation of the chimeric HIV-$gp140_{TM}$ by VLP binding assay. gp160- and $gp140_{TM}$-pseudotyped fluorescent GFP-VLPs were mixed with human PBMC for 1h at 4°C after pre-incubation or not with 2G12 neutralizing antibody during 1h at RT. PBMC were then stained with human CD4 and CD8 antibodies, and VLPs binding was evaluated by flow cytometry as GFP+ cells. Dot plots illustrate GFP fluorescence in CD4+ and CD8+ T cells in presence or not of 2G12 neutralizing antibody to block VLP binding. (D) Comparative immunogenicity of gp160- and $gp140_{TM}$-pseudotyped VLPs. BALB/c mice (n=10 per group) were immunized twice at two-week interval by subcutaneous route with gp160- or $gp140_{TM}$-VLPs mixed with alum. Two weeks after the last injection, HIV-specific T cell responses were measured in spleen by TNFα ICCS (up panel) and HIV-specific IgG antibodies were quantified in serum by gp140-

specific ELISA. ***; p<0.001; Mann-Whitney, compared to controls or between the two indicated groups.

Figure S2: IFNγ responses of memory CD4+ and CD8+ T-cell following vaccination. (A-C) Influence of the immunization routes on systemic and mucosal immune responses in pVLP/VLP prime-boost strategy**.** (A) Immunization protocol. BALB/c mice (n=6 per group) were immunized twice at two-week interval with HIV-pVLPs by ID+EP or IN route of immunizations, then boosted twice with HIV-VLPs by SC or IVag routes respectively. IFNγ-secreting T cells were monitored by intracellular cytokine staining (ICCS) after specific restimulation of cells from spleen, para-aortic lymph nodes (paLN) and vaginal mucosa in memory CD4+ (B) and CD8+ T-cells (C). (D-F) Influence of the administration route for pVLP immunization. (D) Immunization protocol. BALB/c mice (n=6 per group) were immunized twice at two-week interval with HIV-pVLPs by ID+EP or IN route of immunization, then boosted twice with HIV-VLPs by IVag route. IFNγ-secreting T cells were monitored by intracellular cytokine staining (ICCS) after specific restimulation of cells from spleen, para-aortic lymph nodes (paLN) and vaginal mucosa in memory CD4+ (E) and CD8+ T-cells (F). (G-I) Influence of the particulate form of the antigen on systemic and mucosal immunity in prime-boost strategy. (G) Immunization protocol. BALB/c mice (n=6 per group) were immunized twice at two-week interval by intranasal injection (IN) either with gp140-DNA or HIV-pVLPs and then boosted twice by intravaginal immunizations with gp140 recombinant proteins or HIV-VLPs respectively. IFNγ-secreting T cells were monitored by intracellular cytokine staining (ICCS) after specific restimulation of cells from spleen, para-aortic lymph nodes (paLN) and vaginal mucosa in memory CD4+ (H) and CD8+ T-cells (I). Data represent two independent experiments (A and G) or pooled data of two independent experiments (D). *, p<0.05; **, p<0.01; ***, p<0.001; Mann-Whitney,

compared to controls or between the two indicated groups. For the analysis of CD8+ memory T-cells, we are able to analyse secretion in spleen and paLN but not in vaginal mucosa due to too low CD8+ cells in the mucosa.

Figure S3: Influence of the administration route for pVLP immunization. (A) Immunization protocol. BALB/c mice (n=8 per group) were immunized twice at two weeks interval with HIV-pVLPs either by IN or ID+EP route of immunization. HIV-T and B specific immune responses were analyzed two weeks after the last immunization. (B) Specific T-cell responses were evaluated by IFNγ ELISPOT in spleen, para-aortic lymph nodes (paLN) and vaginal mucosa. (C) Specific IgG and IgA antibody responses were assessed by ELISA in serum. (D) Specific IgG- and IgA-secreting B-cells were monitored by B-cell ELISPOT in vaginal mucosa (3 pools of 2 mice per group). (E) Comparative *in vivo* DNA expression after IN and ID+EP administration. Luciferase-encoding DNA expression was evaluated 3 days after IN or ID+EP delivery using *in vivo* imaging system (IVIS) (n=4 per group).

Figure S4: Influence of the particulate form of antigen for intranasal priming. (A) Immunization protocol. BALB/c mice (n=10 per group) immunized twice at days 0 and 7 by IN route with HIV-DNA or HIV-pVLPs. Germinal center reactions were analyzed at day 10 in paLN. (B) Absolute cell numbers of paLN in immunized and control mice. (C-D) T_{FH} immune response. (C) Dot plots representing CXCR5+PD1+ follicular T cells among CD4+ T cells. (D) % of T_{FH} cells characterized as CD4+CXCR5+PD1+FoxP3-Bcl6+ among CD4+ T cells and activation state illustrated by ICOS MFI in T_{FH}. (E) Dot plots representing CD95+GL7+ GCB among CD19+IgD- B cells. (F) % of GCB characterized as CD19+IA/E+IgD-CD95+GL7+ among CD19+ B cells. (G) Linear correlation between T_{FH} and GCB absolute numbers in immunized and control mice. (H) Immunization protocol. BALB/c mice (n=6 per group) were immunized twice at two-

week interval with HIV-pVLPs or DNA by IN route of immunization and HIV-specific immune responses were analyzed two weeks after the last immunization. (I,J) GP140-specific IgG and IgA antibody productions were evaluated by ELISA in sera (I) and BAL (J). (*, $p<0.05$; **, $p<0.01$; ***, $p<0.001$, Mann-Whitney, compared to controls or between the two indicated groups; Data represent pooled results of two different experiments.)

Figure S5: Long-term immune responses in mice vaccinated with IN pVLP/IVag VLP prime-boost strategy. (A) Immunization protocol. BALB/c mice (n=5 per group) were primed two times at two-week intervals with HIV-pVLPs by intranasal route and then boosted twice at two-week intervals with HIV-VLPs by intravaginal route. At W60, mice were additionally boosted with HIV-VLPs by intravaginal route. (B) Concentrations of IgG and IgA antibodies were measured in serum and vaginal washes by ELISA at week 59 and week 61 to determine the impact of the late boost on the humoral immune response. (C) Breadth of the antibody response was evaluated by an epitope mapping assay using HIV-gp140 specific linear overlapping peptides. Specific responses against V1V2 loop, CD4bs, MPER region, V3 loop and α4β7bs were represented at week 8. As controls, MPER-specific mAb (2F5) and sera from influenza-immunized mice (F1, F2) were used. (*, $p<0.05$; **, $p<0.01$; ***, $p<0.001$, Mann-Whitney, compared to controls or between the two indicated groups)

Figure S6: Systemic and mucosal immunity induced in C57BL/6 or BALB/c mice after pVLP/VLP prime-boost strategy. (A) Immunization protocol. BALB/c mice or C57BL/6 mice (n=6 per group) were immunized at two-week intervals by two primes with HIV-pVLPs injected intranasally and two boosts with HIV-VLPs, injected by intravaginal route. HIV-specific T- and B-cell immune responses were analyzed two weeks after the last immunization. (B) Concentrations of IgG and IgA antibodies were

measured in serum and vaginal washes by ELISA. (C) HIV-specific systemic and mucosal memory T-cell immune responses. IFNγ- and TNFα-secreting T cells were monitored by ICCS after specific antigen restimulation of cells from spleen, para-aortic lymph nodes (paLN) and vaginal mucosa. (D) Humoral IgG1/IgG2 ratio in serum was evaluated after ELISA. IgG2a antibodies were revealed for BALB/c mice and IgG2b antibodies were revealed for C57BL/6 mice, in order to determine the Th2/Th1 balance of the humoral response. (*, $p<0.05$; **, $p<0.01$; ***, $p<0.001$; Mann-Whitney, compared to controls or between the two indicated groups)

Figure S7: Germinal center response in C57BL/6 or BALB/c mice after intravaginal delivery of HIV-VLP. (A) Immunization protocol. BALB/c mice or C57BL/6 mice (n=5 per group) were immunized twice at day 0 and day7 by IVag route with HIV-VLPs. Germinal center reactions were analyzed at day 10 in paLN. (B) Absolute cell numbers of paLN in immunized and control mice. (C-D) T_{FH} immune response. (C) % of GCB characterized as CD19+IA/E+IgD-CD95+GL7+ among CD19+ B cells. (D) % of T_{FH} cells characterized as CD4+CXCR5+PD1+FoxP3-Bcl6+ among CD4+ T cells and activation state illustrated by ICOS MFI in T_{FH}. (E) TfH/TFR ratio using absolute number of each cell type were evaluated. (F) Linear correlation between T_{FH} and GCB absolute numbers in immunized and control mice. (*, $p<0.05$; **, $p<0.01$; ***, $p<0.001$, Mann-Whitney, compared to controls or between the two indicated groups)

Figure S8: Influence of the PEI-formulation on DNA expression after intranasal delivery. (A) Immunization protocol. BALB/c mice (n=2) were injected once intranasaly with Luciferase encoding plasmid DNA formulated either with Jet- or Poly-PEI. DNA expression was analyzed over 2 weeks using the In Vivo Imaging System (IVIS spectrum). (B,C) Kinetics of bioluminescence. The average radiance of luminescence

was measured at days 3, 5, 7 and 14. Data represent the kinetic of DNA expression (mean ±SD) and corresponding images observed using IVIS at different time points are shown in C.

Figure S1

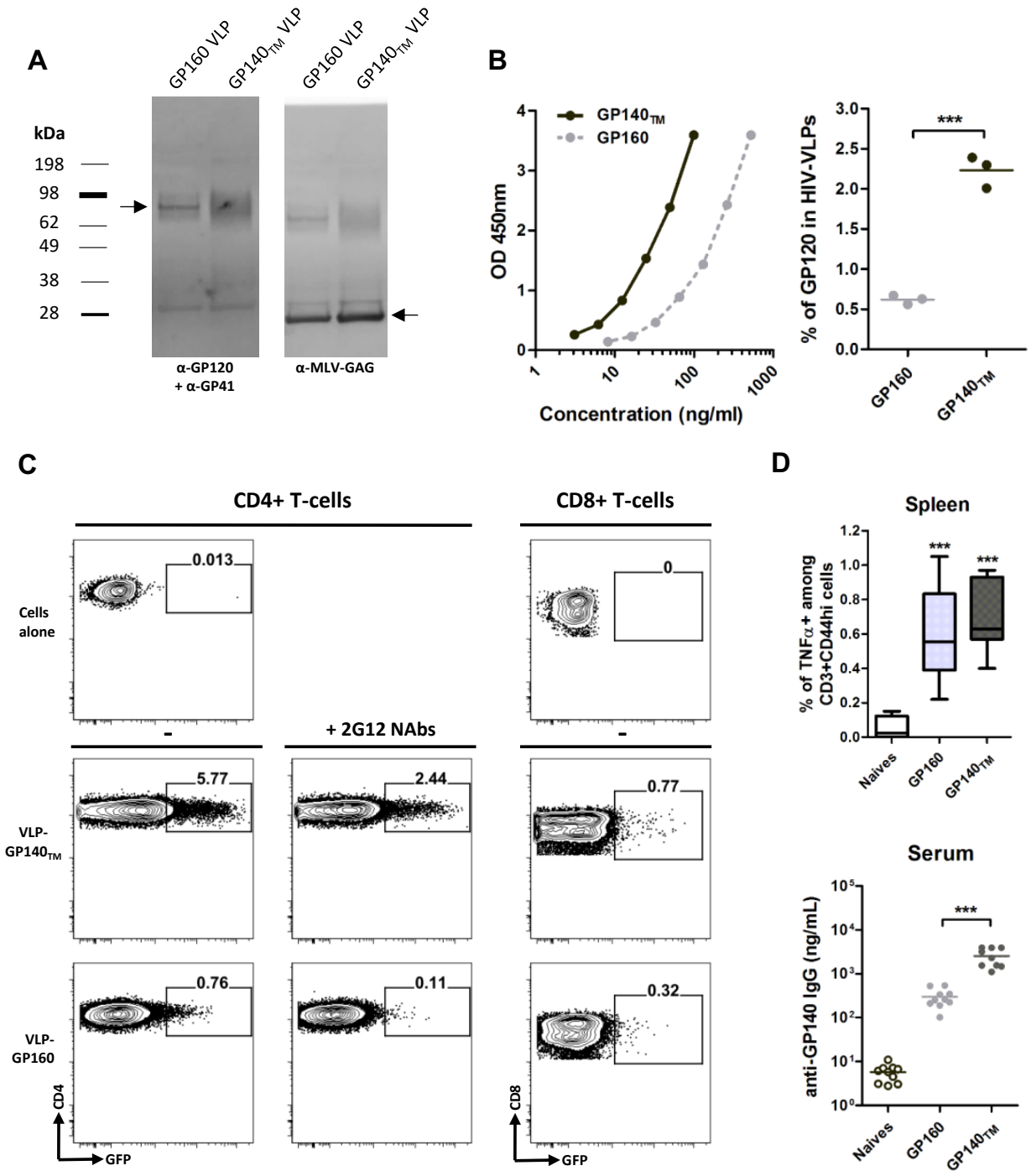
A
GP160 VLP
GP140TM VLP
GP160 VLP
GP140TM VLP
kDa
198
98
62
49
38
28
α-GP120
+ α-GP41
α-MLV-GAG
B
GP140TM
GP160
OD 450nm
Concentration (ng/ml)
% of GP120 in HIV-VLPs
***
GP160
GP140TM
C
CD4+ T-cells
CD8+ T-cells
Cells alone
+ 2G12 NAbs
0.013
0
5.77
2.44
0.77
0.76
0.11
0.32
VLP-GP140TM
VLP-GP160
CD4
CD8
GFP
D
Spleen
% of TNFα+ among CD3+CD44hi cells
Naives
GP160
GP140TM
Serum
anti-GP140 IgG (ng/mL)

Figure S2

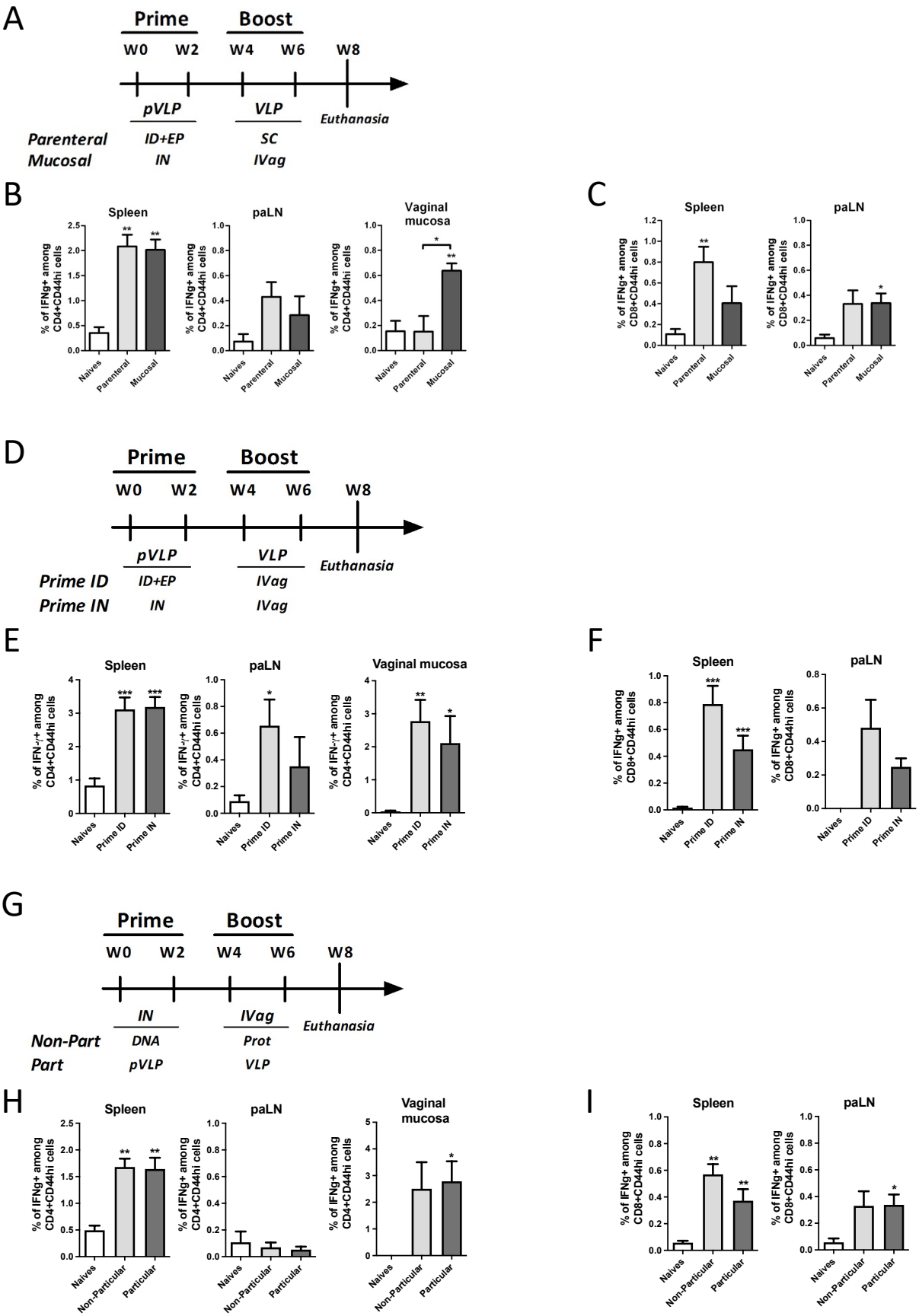
A
Prime
Boost
W0
W2
W4
W6
W8
pVLP
VLP
Euthanasia
Parenteral
ID+EP
SC
Mucosal
IN
IVag
B
Spleen
paLN
Vaginal mucosa
% of IFNg+ among CD4+CD44hi cells
Naives
Parenteral
Mucosal
C
Spleen
paLN
% of IFNg+ among CD8+CD44hi cells
D
Prime
Boost
W0
W2
W4
W6
W8
pVLP
VLP
Euthanasia
Prime ID
ID+EP
IVag
Prime IN
IN
IVag
E
Spleen
paLN
Vaginal mucosa
% of IFN-γ+ among CD4+CD44hi cells
Naives
Prime ID
Prime IN
F
Spleen
paLN
% of IFNg+ among CD8+CD44hi cells
G
Prime
Boost
W0
W2
W4
W6
W8
IN
IVag
Euthanasia
Non-Part
DNA
Prot
Part
pVLP
VLP
H
Spleen
paLN
Vaginal mucosa
% of IFNg+ among CD4+CD44hi cells
Naives
Non-Particular
Particular
I
Spleen
paLN
% of IFNg+ among CD8+CD44hi cells

Figure S3

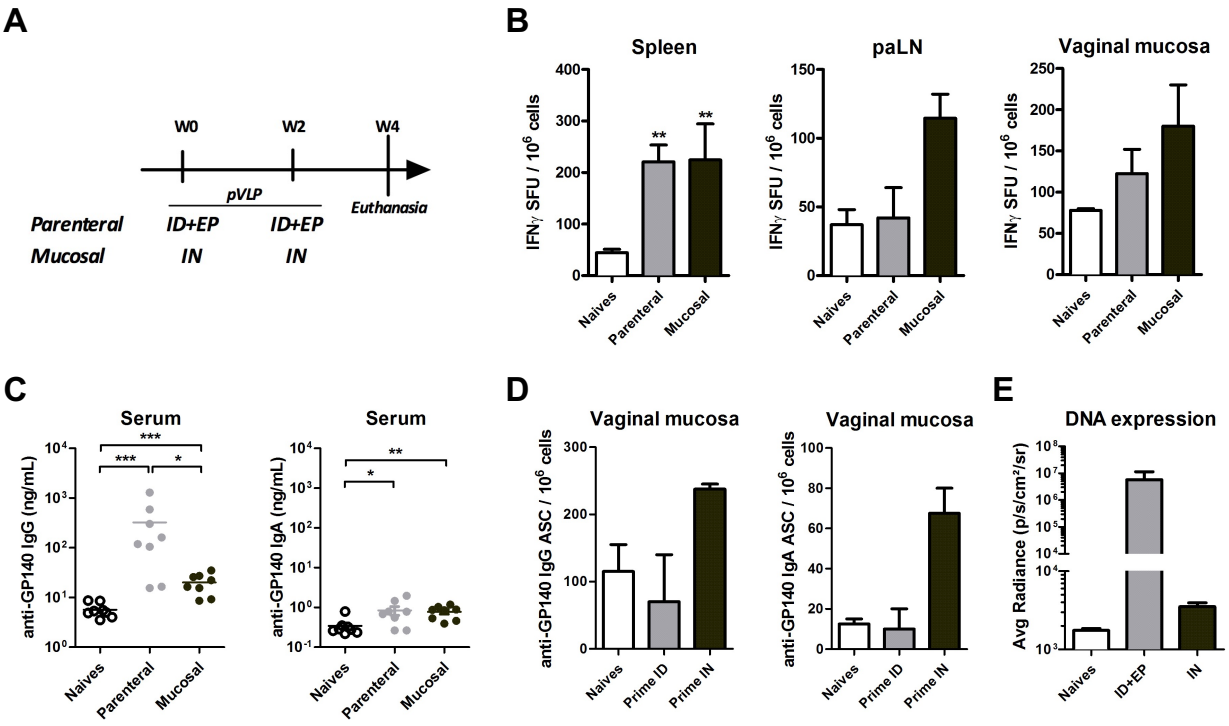
A
W0
W2
W4
pVLP
Euthanasia
Parenteral
ID+EP
ID+EP
Mucosal
IN
IN
B
Spleen
paLN
Vaginal mucosa
IFNγ SFU / 10^6 cells
Naives
Parenteral
Mucosal
C
Serum
anti-GP140 IgG (ng/mL)
Serum
anti-GP140 IgA (ng/mL)
D
Vaginal mucosa
anti-GP140 IgG ASC / 10^6 cells
Vaginal mucosa
anti-GP140 IgA ASC / 10^6 cells
Prime ID
Prime IN
E
DNA expression
Avg Radiance (p/s/cm²/sr)
ID+EP
IN

Figure S4

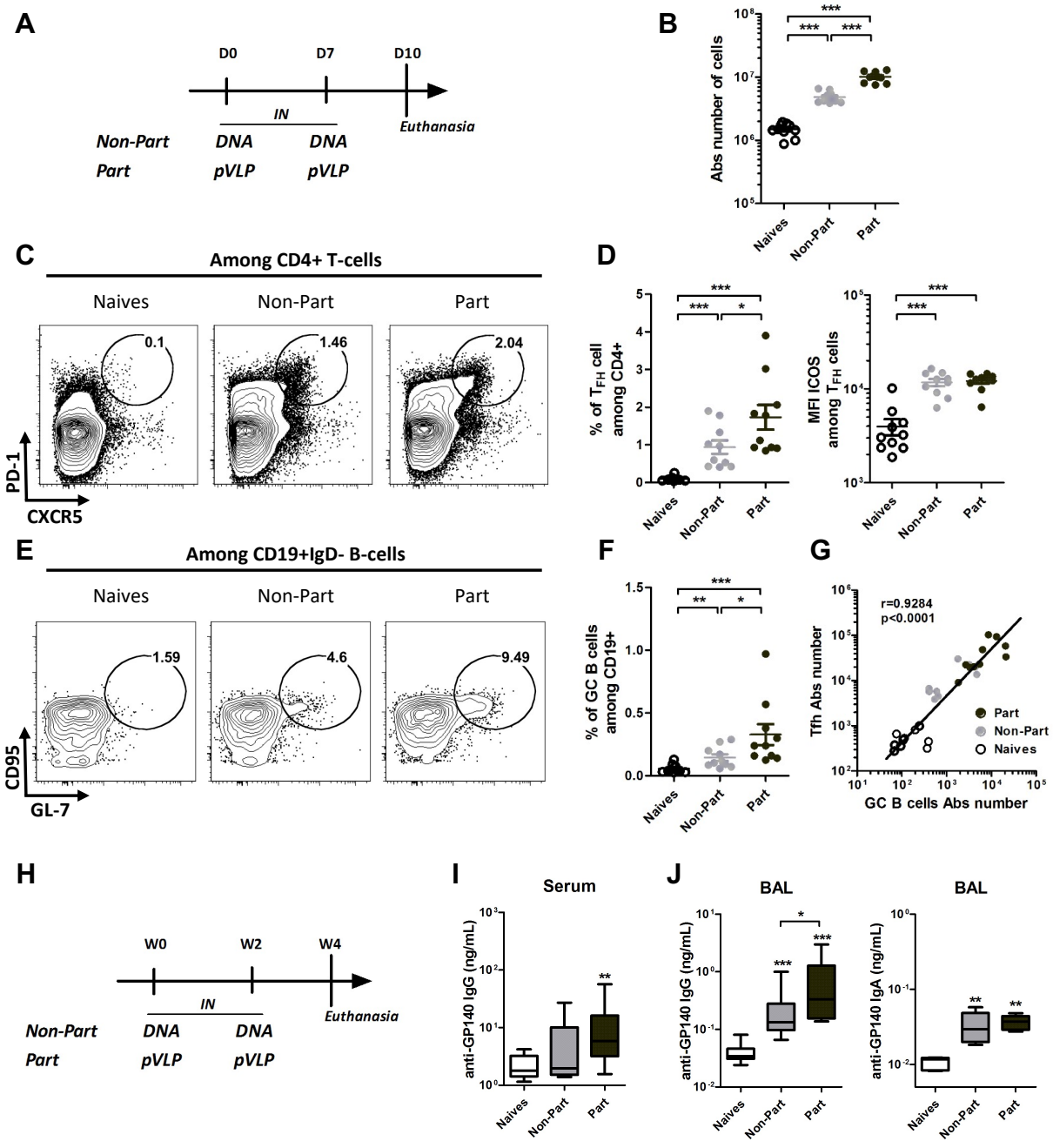
A
D0
D7
D10
IN
Euthanasia
Non-Part DNA DNA
Part pVLP pVLP
B
Abs number of cells
Naives
Non-Part
Part
C
Among CD4+ T-cells
Naives
Non-Part
Part
0.1
1.46
2.04
PD-1
CXCR5
D
% of TFH cell among CD4+
MFI ICOS among TFH cells
E
Among CD19+IgD- B-cells
1.59
4.6
9.49
CD95
GL-7
F
% of GC B cells among CD19+
G
r=0.9284
p<0.0001
Tfh Abs number
GC B cells Abs number
Part
Non-Part
Naives
H
W0
W2
W4
IN
Euthanasia
Non-Part DNA DNA
Part pVLP pVLP
I
Serum
anti-GP140 IgG (ng/mL)
J
BAL
anti-GP140 IgG (ng/mL)
BAL
anti-GP140 IgA (ng/mL)

Figure S5

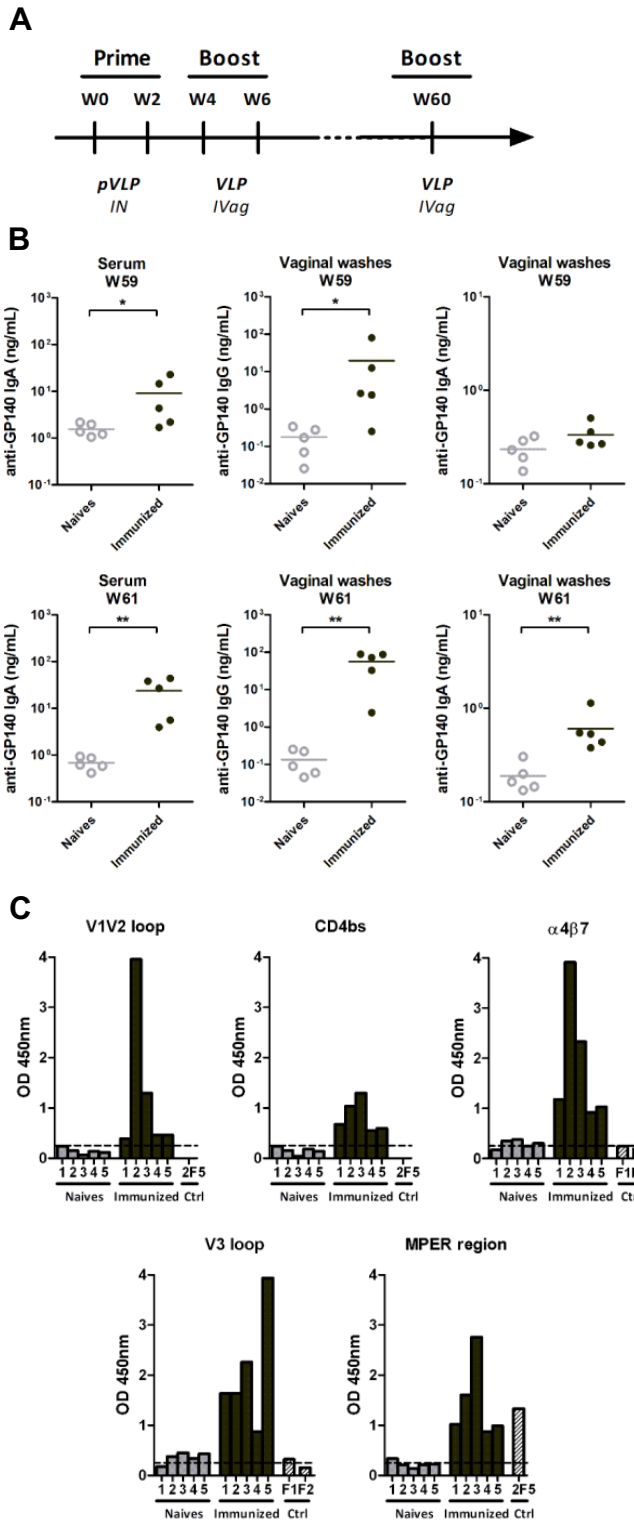
A
Prime
Boost
Boost
W0
W2
W4
W6
W60
pVLP
IN
VLP
IVag
VLP
IVag
B
Serum W59
Vaginal washes W59
Vaginal washes W59
Serum W61
Vaginal washes W61
Vaginal washes W61
anti-GP140 IgA (ng/mL)
anti-GP140 IgG (ng/mL)
Naives
Immunized
C
V1V2 loop
CD4bs
α4β7
V3 loop
MPER region
OD 450nm
1 2 3 4 5
2F5
F1F2
Naives
Immunized
Ctrl

Figure S6

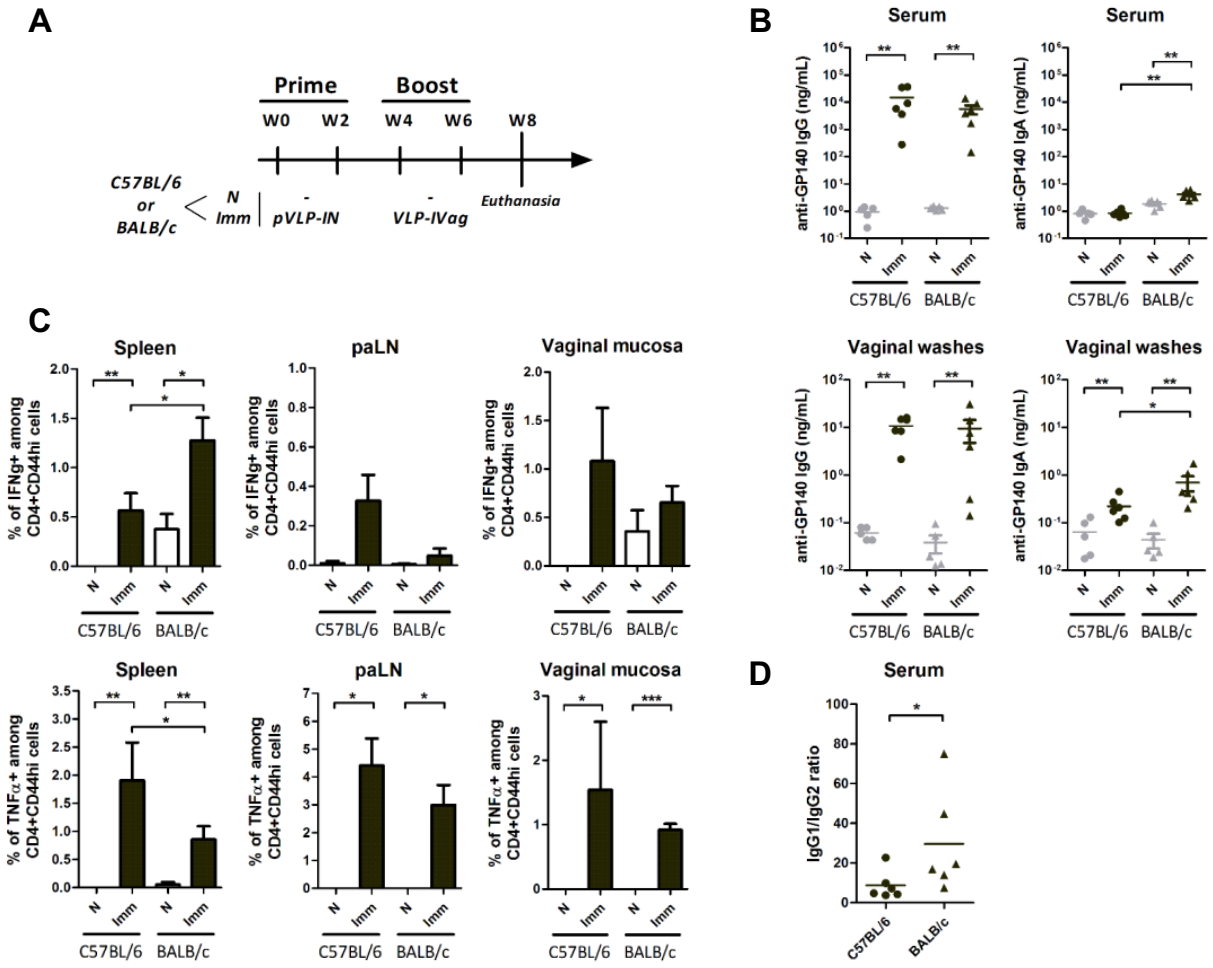
A
Prime
Boost
W0
W2
W4
W6
W8
C57BL/6
or
BALB/c
N
Imm
pVLP-IN
VLP-IVag
Euthanasia
B
Serum
anti-GP140 IgG (ng/mL)
anti-GP140 IgA (ng/mL)
Vaginal washes
C57BL/6
BALB/c
C
Spleen
paLN
Vaginal mucosa
% of IFNg+ among CD4+CD44hi cells
% of TNFα+ among CD4+CD44hi cells
D
IgG1/IgG2 ratio

Figure S7

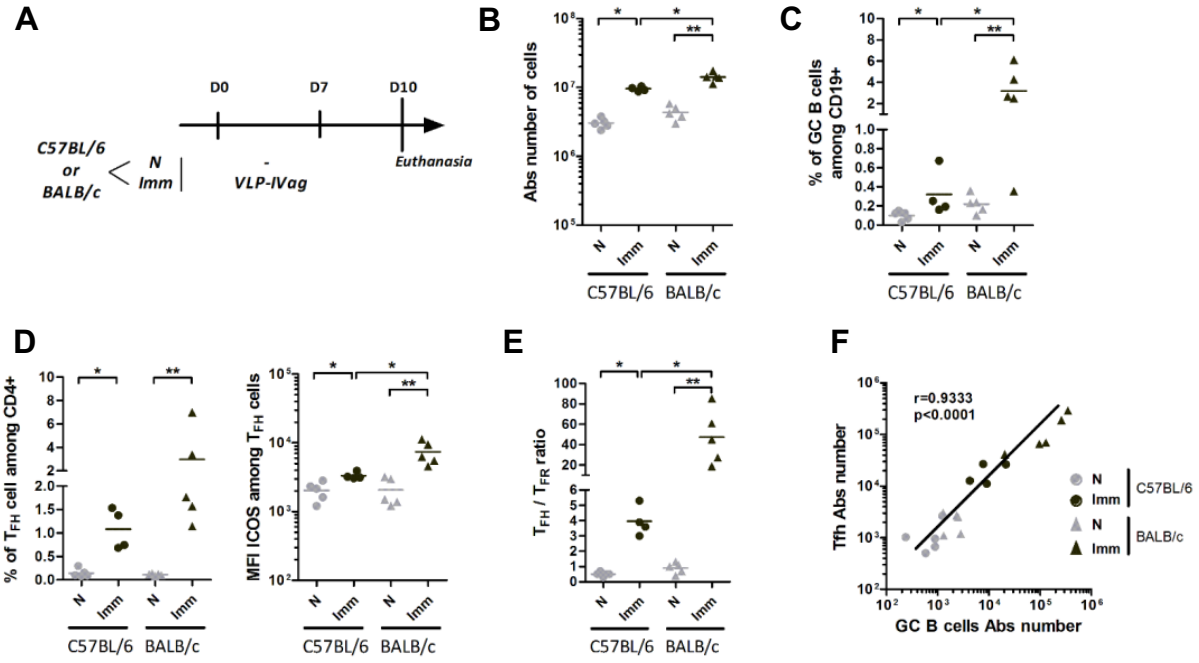
A
D0
D7
D10
C57BL/6
or
BALB/c
N
Imm
-
VLP-IVag
Euthanasia
B
Abs number of cells
C
% of GC B cells
among CD19+
C57BL/6
BALB/c
D
% of TFH cell among CD4+
MFI ICOS among TFH cells
E
TFH / TFR ratio
F
r=0.9333
p<0.0001
Tfh Abs number
GC B cells Abs number
N
Imm
C57BL/6
BALB/c

Figure S8

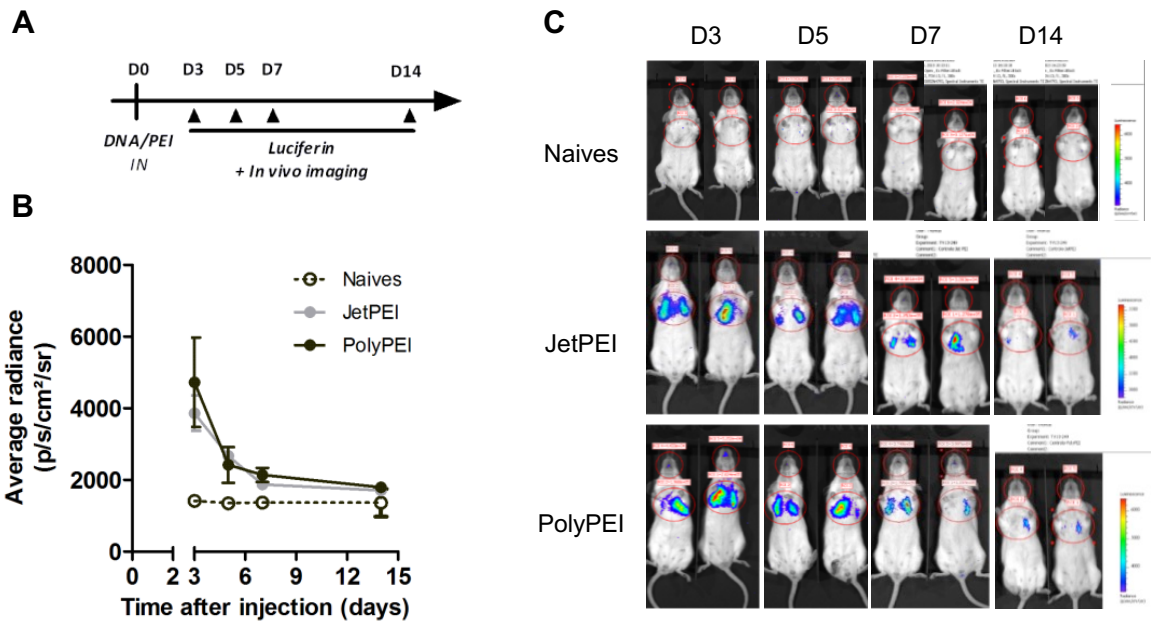
A
D0
D3
D5
D7
D14
DNA/PEI
IN
Luciferin
+ In vivo imaging
B
Average radiance (p/s/cm²/sr)
8000
6000
4000
2000
0
Naives
JetPEI
PolyPEI
0 2 3 6 9 12 15
Time after injection (days)
C
D3
D5
D7
D14
Naives
JetPEI
PolyPEI